



Use of Extremely Bulky Amide Ligands in Main Group Chemistry

Journal:	<i>Chemical Society Reviews</i>
Manuscript ID:	CS-REV-06-2015-000513.R1
Article Type:	Review Article
Date Submitted by the Author:	05-Aug-2015
Complete List of Authors:	Kays, Deborah; University of Nottingham, School of Chemistry

Submitted to *Chemical Society Reviews*

Extremely Bulky Amide Ligands in Main Group Chemistry

Deborah L. Kays

School of Chemistry, University of Nottingham, University Park, Nottingham, UK NG7 2RD.

Fax: +44 115 9513555. E mail: Deborah.Kays@nottingham.ac.uk

Abstract: The search for extremely sterically demanding monodentate amide ligands to access main group complexes in low-coordination numbers and highly reactive bonding modes is an area of intense research interest. The recent development of three classes of sterically demanding, monodentate amide ligands – the *m*-terphenyl anilides $[N(R)\{C_6H_3Ar_{2,6}\}]^-$ (Ar = aryl, R = H, methyl, silyl), substituted carbazol-9-yl and the extremely bulky amides $[N(R)(Ar')]^-$ (Ar' = 2,6- $\{C(H)Ph_2\}$ -4-R'-C₆H₂, R = silyl, aryl, silyloxy, R' = alkyl) is facilitating the isolation of stable species with new coordination modes for the main group elements. These compounds are of fundamental importance not only from the investigation of their structure and bonding, but also the investigation of their reactivity highlights the potential for small molecule activation chemistry under mild conditions and applications in catalysis. This review reports on the recent developments for these compounds with emphasis on their synthesis, structure and reactivity.

1. Introduction

Amides of the general formula $[\text{NR}^1\text{R}^2]^-$ (R^1 and R^2 = alkyl, aryl, silyl and substituents which can also be incorporated into a heterocyclic ring system) are highly useful ligands for the main group elements as the variation of the R groups can impart differing steric and electronic properties, and facilitate the incorporation of intramolecular donors.¹⁻³ It is without a doubt that the pioneering sterically demanding amide is the *bis*-trimethylsilylamide ligand $[\text{N}(\text{SiMe}_3)_2]^-$, which has stabilised a range of main group complexes featuring novel coordination modes. The *s*- and *p*-block chemistry of this ligand has been comprehensively reviewed in recent papers by Coles.^{4,5} The $[\text{N}(\text{SiMe}_3)_2]^-$ ligand is particularly useful due to the ease of synthesis of the anion, and the resulting stability of complexes due to ligand bulk and lack of β -hydrogens. It can adopt terminal or bridging coordination modes in complexes. In the quest for the stabilisation of lower coordination numbers and more challenging species, researchers over the years have been looking towards increasing the steric bulk of amide ligands through the utilisation of substituents with greater steric demands, such as in the 2,2,6,6-tetramethylpiperidide (Tmp),⁶ $[\text{N}(\text{SiMe}_3)(\text{Mes})]^-$ (Mes = 2,4,6-Me₃C₆H₂),⁷ $[\text{N}(\text{SiR}_3)(\text{Dipp})]^-$ (Dipp = 2,6-^{*i*}Pr₂C₆H₃, R = Me, Ph),⁸ $[\text{N}(\text{SiMe}_3)(\text{Mes}^*)]^-$ (Mes = 2,4,6-^{*t*}Bu₃C₆H₂),⁹ and $[\text{N}(\text{SiPh}_3)(\text{Ad})]^-$ (Ad = adamantyl)¹⁰ ligands. However, these bulky monodentate ligands generally provide less protection towards common issues facing highly reactive main group complexes such as disproportionation and oligomerisation than their bulky bidentate counterparts *e.g.* amidinates, guanidates, β -diketiminates and the doubly reduced diazabutadienes.¹¹⁻²⁵ Thus, the search for significantly more sterically demanding monodentate amide ligands to stabilise *s*- and *p*-block complexes in low-coordination numbers and/or hitherto unknown oxidation states is an area of intense research interest. This is particularly relevant given the recent success of the sterically demanding aryl ligands, *m*-terphenyls, which have been used in the isolation and investigation of a range of unusual and

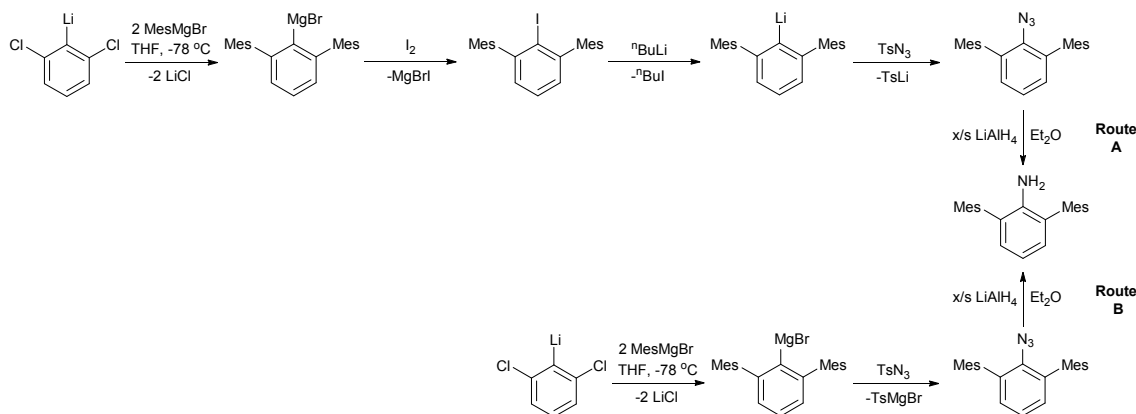
highly reactive bonding modes for low-coordinate main group and transition metal complexes, due to their versatility and excellent steric hindrance.²⁶

Increasing the steric hindrance provided by monodentate amide ligands is generally being accomplished through the incorporation of even more sterically demanding aryl and silyl substituents, such as in the *m*-terphenyl anilides $[N(R)\{C_6H_3Ar_2-2,6\}]^-$ (Ar = aryl, R = H, methyl, silyl) and the extremely bulky $[N(R)(Ar')]^-$ (Ar' = 2,6- $\{C(H)Ph_2\}$ -4-R'-C₆H₂, R = silyl, aryl, silyloxy, R' = alkyl) ligands, and also through the use of rigid nitrogen-based frameworks substituted with bulky alkyl or aryl substituents, *e.g.* 1,3,6,8-tetra-*tert*-butylcarbazol-9-yl or 1,8-diaryl-3,6-di(*tert*-butyl)carbazol-9-yl ligands. These extremely bulky amide ligands are facilitating the isolation of stable species with low-coordinate and highly reactive bonding modes for the main group elements, including three-coordinate Group 2 complexes, monomeric Group 13 M(I) amides, two-coordinate hydrido-germylenes and stannylenes, Group 14 complexes featuring E–E single and multiple bonds, cationic Group 15 complexes and dipnictines. Furthermore, reactivity investigations are highlighting the potential use of some of these compounds in small molecule activation chemistry and catalysis. The latest advances are showing how these ligands are challenging the more ubiquitous *m*-terphenyls in terms of their steric bulk and tunability. The main group chemistry of these three families of ligands will be explored in turn in this review.

2. *m*-Terphenyl Anilide and Imide Ligands

Although *m*-terphenyl ligands have been utilised in the stabilisation of highly reactive main group complexes since the early 1990's, their anilide counterparts $[N(R)\{C_6H_3Ar_2-2,6\}]^-$ (R = H, Me, SiMe₃) did not come into use until around a decade later. Their utilisation is still extremely limited compared to the *m*-terphenyls, but they are showing that they are versatile ligands for the main group elements, and can provide a degree of tuning with regards

to the steric pocket they provide. The anilines were originally synthesised through a multi-step process (Route A, Scheme 1);²⁷ however, this has been subsequently improved by Power and co-workers through a modified two-pot process (Route B, Scheme 1).²⁸ To increase the steric bulk of these compounds one of the nitrogen-substituted protons can be substituted with a trimethylsilyl or methyl group providing 2,6-Mes₂C₆H₃N(SiMe₃)H or 2,6-Mes₂C₆H₃N(Me)H, respectively. Given that the *m*-terphenyl-based amides and imides are closely related, and are often synthesised from the anilines or anilides there will also be some limited discussion of the main group imides in this Section.



Scheme 1 Synthesis of 2,6-Mes₂C₆H₃NH₂ via a multistep process (Route A) and by a modified two-pot process (Route B).²⁸

2.1 s-Block Complexes

A range of lithium complexes of *m*-terphenyl anilide ligands of varying steric bulk have been developed to afford main group (see Sections below) and transition metal complexes through metathesis reactions.²⁹ The *m*-terphenyl lithium salts are generally synthesised through reaction with *n*BuLi.²⁸ The solid state structure of [2,6-Mes₂C₆H₃N(Li)Me]₂ (**1**) reveals an amide-bridged dimer with a planar Li₂N₂ core and unusual two-coordinate lithium centres. The synthesis and structure of the potassium salt of the

triisopropylphenyl-substituted anilide 2,6-Trip₂C₆H₃N(H)K(OEt)₂ (**2**) has been reported; this compound has been used in the synthesis of neodymium complexes.³⁰

2.2 Group 13 Complexes

The reaction between the azide 2,6-Dipp₂C₆H₃N₃ and the Al(I) β-diketiminato {HC[(CMe)(NDipp)]₂}Al afforded isomers **3A** and **3B** (Figure 1) derived from an unprecedented intramolecular addition reaction of the Al=N bond and rearrangement of the parent imide {HC[(CMe)(NDipp)]₂}Al=NC₆H₃Dipp₂-2,6 (**3**).³¹ Although these isomers were initially present in approximately equal amounts, the amount of **3A** was found to diminish in solution, with concomitant increase in **3B**. The thermal stability of these three isomers is **3** < **3A** < **3B**. Highlighting the unusual nature of this reactivity, the isolation of products **3A** and **3B** is in contrast to the triisopropylphenyl analogues – where the aluminium and gallium imides {HC[(CMe)(NDipp)]₂}M=NC₆H₃Trip₂-2,6 (M = Al **4**, Ga **5**) can be stabilised as monomeric species in the solid state.³² Related monomeric, two-coordinate imides 2,6-Dipp₂C₆H₃M=NC₆H₃(2,6-Me-4-^tBuC₆H₂)₂-2,6 (M = Ga **6**, In **7**) have also been reported.³³ The 2,6-Mes₂C₆H₃-substituted isomer of **3B** has also been used to generate a C–H-activated aluminium hydroxide complex.³⁴

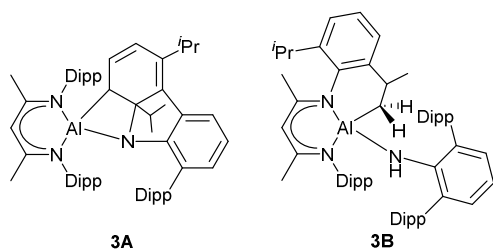


Figure 1 The two isomers **3A** and **3B** formed from the intramolecular addition reaction of {HC[(CMe)(NDipp)]₂}Al=NC₆H₃Dipp₂-2,6 (**3**).³¹

An iminoborane 2,6-Mes₂C₆H₃N≡BTmp (**8**; Figure 2) was synthesised from the reaction between the amides 2,6-Mes₂C₆H₃N(H)B(X)Tmp (X = Cl **9**, Br **10**) and Na[N(SiMe₃)₂].³⁵ The iminoborane was identified by the ¹¹B NMR chemical shift of δ_B 10.6 ppm and the infrared spectrum which showed two bands at 2037 and 1982 cm⁻¹, due to the ν(B≡N) for the ¹⁰B and ¹¹B isotopologues. The solid state structure of **8** exhibits a near linear C(terphenyl)–N–B–N(Tmp) core and a very short B–N(terphenyl) distance [1.254(3) Å].

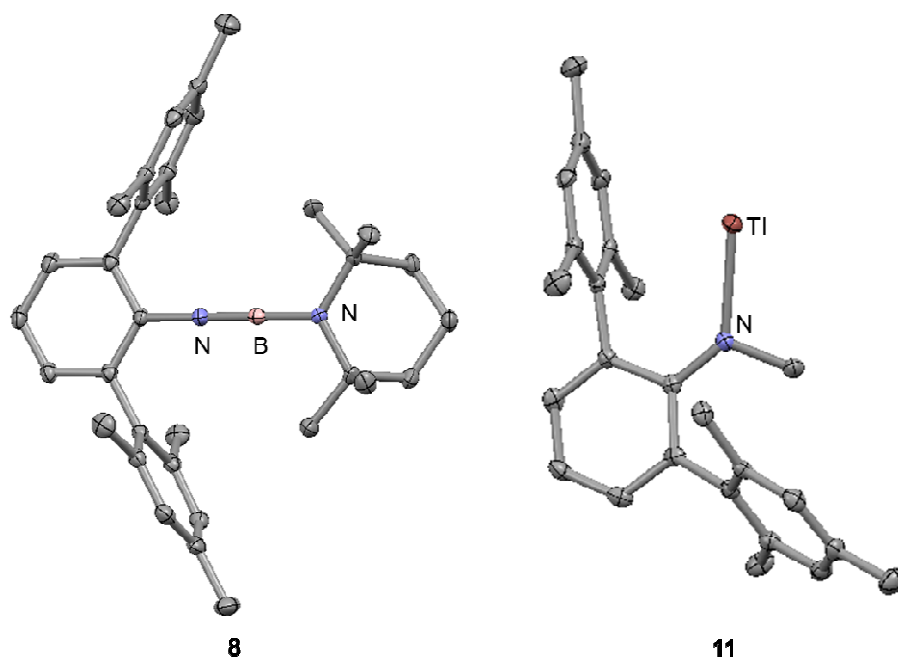


Figure 2 Iminoborane 2,6-Mes₂C₆H₃N≡BTmp (**8**) formed from the reaction between 2,6-Mes₂C₆H₃N(H)B(X)Tmp (X = Cl **9**, Br **10**) and Na[N(SiMe₃)₂]³⁵ and the unassociated Tl(I) amide, 2,6-Mes₂C₆H₃N(Me)Tl (**11**).³⁶

The 2,6-Mes₂C₆H₃N(Me)⁻ ligand has been used to stabilise the unassociated thallium(I) amide, 2,6-Mes₂C₆H₃N(Me)Tl (**11**, Figure 2),³⁶ the steric demands of the *m*-terphenyl anilide affording a monomer in the solid state. This complex has a relatively long Tl–N distance [ave. 2.364(3) Å] and there is an interaction between the thallium centre and one of the flanking mesityl substituents. DFT calculations on a model complex revealed that

this Tl-arene interaction is likely to be weak (in the order of $3.0 \text{ kcal mol}^{-1}$). The first stable monomeric gallium(I) complex $2,6\text{-Mes}_2\text{C}_6\text{H}_3\text{N}(\text{SiMe}_3)\text{Ga}$ (**12**), formed from the reaction between $2,6\text{-Mes}_2\text{C}_6\text{H}_3\text{N}(\text{SiMe}_3)\text{Li}$ (**13**) and “GaI”, features a similar core structure to the Tl complex **11**, but in this case an interaction between the *ipso*-carbon on a flanking mesityl substituent aids in the stabilisation.³⁷ This Ga \cdots C distance is *ca.* 0.6 \AA longer than that of a Ga–C single bond, leaving the gallium essentially one-coordinate. DFT calculations on model complexes suggested that there is a contribution to the structure from a resonance form which possesses a Ga–N π -bond formed from the donation of the nitrogen lone pair to an empty $4p$ orbital on gallium. **12** is of interest as it is isomeric with the relevant imide complex. The reaction between **12** and (*p*-tol)N=N(*p*-tol) (*p*-tol = $4\text{-MeC}_6\text{H}_4$) in toluene solution does not occur, unlike the *m*-terphenyl complex $2,6\text{-Dipp}_2\text{C}_6\text{H}_3\text{Ga}$. **12** does, however, react with the azide $2,6\text{-Mes}_2\text{C}_6\text{H}_3\text{N}_3$ yielding the imide/amide $2,6\text{-Mes}_2\text{C}_6\text{H}_3\text{N}(\text{SiMe}_3)\text{GaN}(\text{C}_6\text{H}_3\text{-Mes}_2\text{-2,6})$ (**14**, Figure 3), with concomitant formation of dinitrogen. This heterocumulene has been likened to a heavier Group 13 element-nitrogen analogue of an allyl anion, but unlike an allyl there is little delocalisation across the N–Ga–N unit.

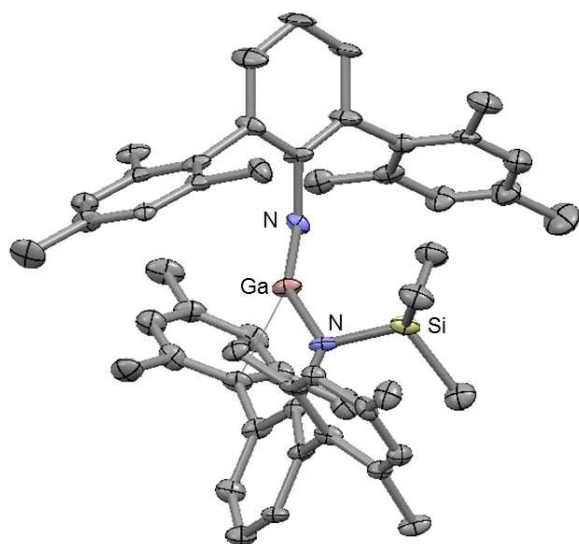


Figure 3 The molecular structure of one of the crystallographically independent molecules of 2,6-Mes₂C₆H₃N(SiMe₃)GaN(C₆H₃-Mes₂-2,6) (**14**), with thermal ellipsoids set at 50%.³⁷ Hydrogen atoms are omitted for clarity.

2.3 Group 14 Complexes

Imides [(2,6-Ar₂C₆H₃)N]²⁻ can stabilise the dichlorosilaimine complexes IPr·Cl₂Si=N(2,6-Ar₂C₆H₃) (IPr = 1,3-*bis*(2,6-diisopropylphenyl)imidazol-2-ylidene, Ar = Dipp **15**, Trip **16**)³⁸ and a silaisonitrile [(2,6-Trip₂C₆H₃)NSi:]₂ (**17**) formed *via* reduction of **16**.^{39,40} Three- and four-coordinate silaimine {CH[(C=CH₂)(CMe)(2,6-^{*i*}Pr₂C₆H₃N)₂]}Si=NC₆H₃-2,6-Trip₂ (**18**) and PhC(N^{*t*}Bu)₂(Cl)SiNC₆H₃-2,6-Trip₂ (**19**) can also be synthesised.⁴¹ The reactions of the lanthanide silylamides Ln{N(SiHMe₂)₂}(THF)₂ with the aniline 2,6-Mes₂C₆H₃NH₂ affords LnN{SiMe₂N(C₆H₃-2,6-Mes₂)₂}₂ (Ln = Ce **20**, Pr **21**), which feature N–Si bonds, the tridentate ligands formed *via* a lanthanide-induced Si–H activation.⁴² Analogous reaction of the more sterically encumbered 2,6-Trip₂C₆H₃NH₂ yields NH{SiMe₂NH(C₆H₃-2,6-Trip₂)₂}₂ (**22**).

The solvent-free reaction between M{N(SiMe₃)₂}₂ and the aniline 2,6-Mes₂C₆H₃NH₂ at elevated temperatures afforded the corresponding imide dimers {M(μ-NC₆H₃Mes₂-2,6)}₂ (M = Ge **23**, Sn **24**, Pb **25**) with concomitant elimination of (Me₃Si)₂NH.⁴³ The reaction between M{N(SiMe₃)₂}₂ and two equivalents of 2,6-Mes₂C₆H₃NH₂ in toluene yielded the rare monomeric *bis*(primary amide) complexes M{N(H)C₆H₃Mes₂-2,6)}₂ (M = Ge **26**, Sn **27**, Pb **28**). The crystal structure of **27** is given in Figure 4. Based on spectroscopic observations an equilibrium is proposed to exist between M{N(H)C₆H₃Mes₂-2,6)}₂ and {M(μ-NC₆H₃Mes₂-2,6)}₂. Dimerisation of the imide units leads to non-planar M₂N₂ rings, with significant folding along the metal-metal axis in **23-25**. For the germanium complex **23** the degree of folding is smaller than for the heavier congeners **24** and **25** (dihedral angle between the two

NM₂ planes in **23** = 172.4° and analogous angle for **24** and **25** = 148.3°). The amide complexes **26-28** possess acute N–M–N angles of 88.6(2)° (**26**), 87.07(8)° (**27**), and 87.47(9)° (**28**), which is rare for the two-coordinate derivatives of these Group 14 metals. The electronic spectra of the complexes feature *n*→*p* transitions, the energy of this decreasing in the sequence Ge > Sn > Pb for both the imide and amide series. This decrease may be due to partial quenching of the HOMO→LUMO transition by strong metal-arene interactions in the Sn and Pb complexes.

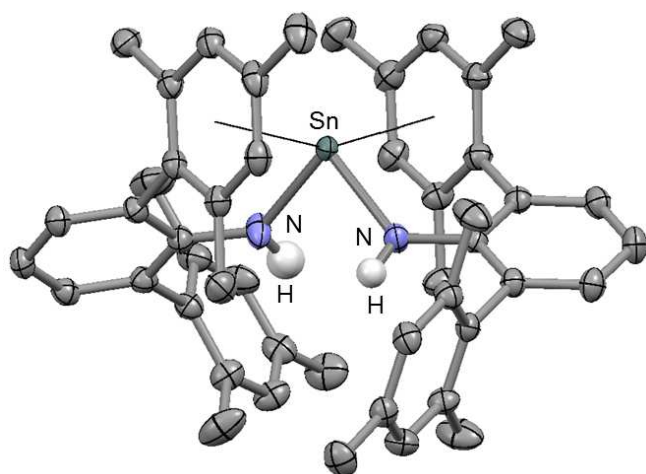


Figure 4 The molecular structure of Sn{N(H)C₆H₃Mes₂-2,6}₂ (**27**), with thermal ellipsoids set at 50%.⁴³ Hydrogen atoms, with the exception of the anilide hydrogens are omitted for clarity.

2.4 Group 15 Complexes

The parent anilide ligand 2,6-Mes₂C₆H₃NH[−] opens up a large area of chemistry involving Group 15 heterocycles. The *cyclo*-1,3-dipnicta-2,4-diazane complexes, which feature a four-membered E₂N₂ ring (E = P **29**, As **30**, Sb **31**, Bi **32**) are formed by the reaction of 2,6-Mes₂C₆H₃N(H)ECl₂ (E = P **33**, As **34**, Bi **35**)⁴⁴⁻⁴⁷ with a base or *via* the reaction between the tin amide **24** and ECl₃ (E = Sb, Bi).⁴⁸ **29** is formed in a mixture of *cis* and *trans* isomers.^{47,49} For the amido(chloro)phosphine complex, if a large excess of the reagents

triethylamine and PCl_3 are used it is possible to afford the diphosphine complex 2,6-Mes₂C₆H₃N(PCl₂)₂ (**36**), which can undergo further metathesis chemistry.⁴⁷ The phosphorus compound **29** can be formed using NEt_3 as the base, but for the arsenic and bismuth analogues only DBU (DBU = 1,8-diazabicyclo[5.4.0]undec-7-ene) has been successfully employed thus far. In the case of arsenic complex **30** the choice of reaction conditions and base is very important: use of DBU at warmer temperatures affords a complex mixture featuring 2-*m*-terphenyl-amino-2-arsa-3,7-diazatricyclo[5.4.1.0^{3,12}]dodec-3(12)-enyliumchloride (**37**), and the use of LDA (lithium diisopropylamide) affords 2,6-Mes₂C₆H₃N(H)As(Cl)N^{*i*}Pr₂ (**38**).

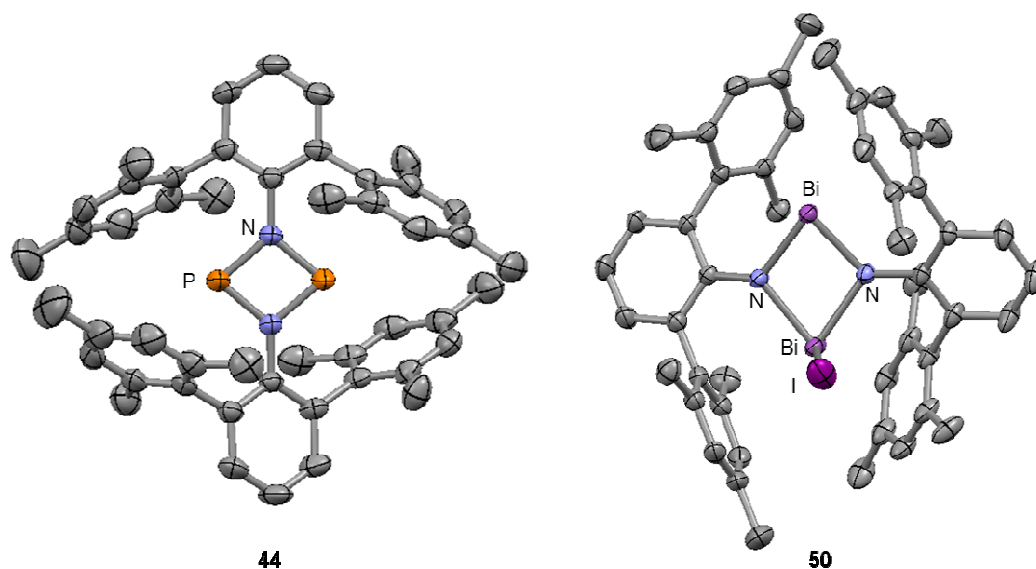
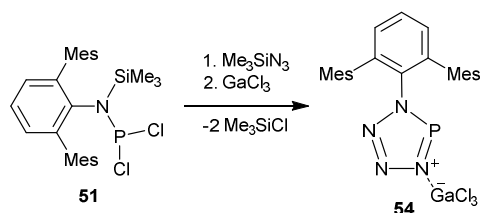


Figure 5 The molecular structures of the stable biradicaloid $[\text{P}(\mu\text{-NC}_6\text{H}_3\text{Mes}_2\text{-2,6})]_2$ (**44**) and the cationic part of $[(2,6\text{-Mes}_2\text{C}_6\text{H}_3\text{N})_2\text{Bi}_2\text{I}]^+[\text{B}(\text{C}_6\text{F}_5)_4]^-$ (**50**), with thermal ellipsoids set at 50%.^{48,50} Hydrogen atoms omitted for clarity.

Complexes **29-32** can be used in the synthesis of 1-chloro-*cyclo*-1,3-dipnicta-2,4-diazanium cations: $[(2,6\text{-Mes}_2\text{C}_6\text{H}_3\text{N})_2\text{P}_2\text{Cl}]^+[\text{GaCl}_4]^-$ (**39**),⁴⁴ $[(2,6\text{-Mes}_2\text{C}_6\text{H}_3\text{N})_2\text{As}_2\text{Cl}]^+[\text{X}]^-$ ($[\text{X}]^- = [\text{GaCl}_4]^-$ **40**, OTf^- **41**, $\text{OTf}^- = \text{SO}_3\text{CF}_3^-$) and⁴⁵ $[(2,6\text{-Mes}_2\text{C}_6\text{H}_3\text{N})_2\text{E}_2\text{Cl}]^+[\text{GaCl}_4]^-$ (E = Sb **42**, Bi **43**),⁴⁸ 1-azido-*cyclo*-1,3-dipnicta-2,4-diazanium cations (E = P **44**, As **45**)^{44,45} and in

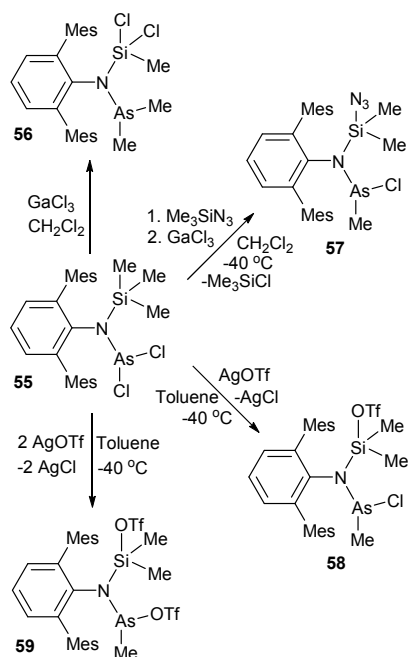
the generation of stable biradicaloids such as $[\text{E}(\mu\text{-NC}_6\text{H}_3\text{Mes}_2\text{-2,6})]_2$ ($\text{E} = \text{P}$ **46** Figure 5, As **47**).^{50,51} Complexes **29** and **46** form a cyclic compound $(2,6\text{-Mes}_2\text{C}_6\text{H}_3\text{N})_2\text{PLi}$ (**48**) which features a four-membered LiPN_2 ring upon reactions with lithium.⁵⁰ The reaction between $(2,6\text{-Mes}_2\text{C}_6\text{H}_3\text{N})_2\text{Bi}_2\text{I}_2$ (**49**) and $\text{Ag}[\text{B}(\text{C}_6\text{F}_5)_4]$ afforded the 1-iodo-*cyclo*-1,3-dibismutha-2,4-diazanium complex $[(2,6\text{-Mes}_2\text{C}_6\text{H}_3\text{N})_2\text{Bi}_2\text{I}]^+[\text{B}(\text{C}_6\text{F}_5)_4]^-$ (**50**) (Figure 5).⁴⁸



Scheme 2 Synthesis of tetrazaphosphole **54**.⁴⁴

The reaction between $2,6\text{-Mes}_2\text{C}_6\text{H}_3\text{N}(\text{SiMe}_3)\text{PCL}_2$ (**51**) and $\text{DBU}/\text{R}_f\text{OH}$ ($\text{R}_f\text{OH} =$ hexafluoroisopropanol) yielded only trace amounts of the *cyclo*-1,3-diphospha-2,4-diazane **29**, with the major products being $2,6\text{-Mes}_2\text{C}_6\text{H}_3\text{N}(\text{H})\text{P}(\text{OR}_f)\text{Cl}$ (**52**) and $2,6\text{-Mes}_2\text{C}_6\text{H}_3\text{N}(\text{H})\text{P}(\text{OR}_f)_2$ (**53**).⁴⁹ The reaction between **51** (which can be regarded as a "disguised" polarophile), the Lewis acid GaCl_3 and Me_3SiN_3 yields a tetrazaphosphole **54** (Scheme 2).⁴⁴ The reaction in the absence of the azide initially yields $2,6\text{-Mes}_2\text{C}_6\text{H}_3\text{N}=\text{PCL}$, which then reacts with GaCl_3 forming the labile $[2,6\text{-Mes}_2\text{C}_6\text{H}_3\text{N}=\text{P}]^+[\text{GaCl}_4]^-$. Subsequent addition of Me_3SiN_3 affords **54**, confirming the existence of the cation. In analogy to this⁴⁴ and a previous phosphorus example,⁵² it was presumed that the $2,6\text{-Mes}_2\text{C}_6\text{H}_3\text{N}(\text{SiMe}_3)\text{AsCl}_2$ (**55**) would generate $2,6\text{-Mes}_2\text{C}_6\text{H}_3\text{N}=\text{AsCl}$ *via* elimination of Me_3SiCl . Thus, **55** was reacted with GaCl_3 in CH_2Cl_2 solution, but instead of the imino(chloro)arsine the methyl/chloride exchange product $2,6\text{-Mes}_2\text{C}_6\text{H}_3\text{N}(\text{SiMeCl}_2)\text{AsMe}_2$ (**56**) was afforded (Scheme 3).⁵³ Changing the synthetic approach to determine whether a [3+2] cyclisation is faster than a methyl/chloride or methyl/azide exchange reaction afforded $2,6\text{-Mes}_2\text{C}_6\text{H}_3\text{N}\{\text{Si}(\text{N}_3)\text{Me}_2\}\text{AsMeCl}$ (**57**), formed *via* migration of a methyl group to arsenic.

Reactions between **55** and AgOTf proceed *via* methyl/triflate exchange, yielding 2,6-Mes₂C₆H₃N{Si(OTf)Me₂}AsMeCl (**58**) and 2,6-Mes₂C₆H₃N{Si(OTf)Me₂}AsMeOTf (**59**), with one and two equivalents of AgOTf, respectively. Calculations indicate that regardless of the Lewis acid, the first reaction step involves chloride abstraction and the intermediate formation of a cationic species with a formal positive charge localised at the nitrogen atom. Hyperconjugation within the molecule gives rise to a long Si–C bond which facilitates the shift of a methyl from Si to As, with concomitant attack of a Lewis basic anion (Cl[−], N₃[−], OTf[−]) on the positively charged Si centre.



Scheme 3 Reactions of the arsenic complex 2,6-Mes₂C₆H₃N(SiMe₃)AsCl₂ (**55**).⁵³

Similar chemistry is observed for the antimony analogue 2,6-Mes₂C₆H₃N(SiMe₃)SbCl₂ (**60**).⁵⁴ Reactions towards the substrates AgOTf, AgN₃, KO^tBu, GaCl₃ and Me₃SiN₃/GaCl₃ proceed *via* triflate/methyl, azide/methyl and chlorine/methyl exchange reactions between the silicon and antimony centres.

Recently, terphenyl ligands have been used to stabilise the disubstituted *N,N*-bis(amido)phosphenium cation $[\{2,6\text{-Mes}_2\text{C}_6\text{H}_3\text{N(H)}\}_2\text{P}]^+$ (**61**) which has been used as a highly sensitive probe for interactions with a number of different anions: F^- , Cl^- , $[\text{CF}_3\text{CO}_2]^-$, OTf^- , $[\text{B}(\text{C}_6\text{F}_5)_4]^-$, $[\text{GaCl}_4]^-$, $[\text{SbF}_6]^-$, $[\text{Al}\{\text{OCH}(\text{CF}_3)_2\}_4]^-$ and $[\text{CHB}_{11}\text{H}_5\text{Br}_6]^-$.⁵⁵ Structural investigations have shown three types of cation-anion interaction within these complexes: (i) polar covalent bonding between the phosphorus and $[\text{X}]^-$ for the small, nucleophilic anions such as F^- , Cl^- and $[\text{CF}_3\text{CO}_2]^-$, (ii) $\text{NH}\cdots\text{Y}$ hydrogen bonds (where Y = the donor atom of the anion) were observed for medium-sized $[\text{X}]^-$, and (iii) weak van der Waals interactions with peripheral H-C_{Mes} atoms were observed for the large, weakly-coordinating anions ($[\text{SbF}_6]^-$, $[\text{Al}\{\text{OCH}(\text{CF}_3)_2\}_4]^-$ and $[\text{CHB}_{11}\text{H}_5\text{Br}_6]^-$) which are too big to fit into the pocket created by the *m*-terphenyl ligands.

2.5 Group 16 Complexes

Terphenyl substituents have been used to stabilise thioaminyll radicals, which have been postulated to have potential use in new magnetic materials. These compounds are remarkably persistent, even in the presence of oxygen and exist in the individual radical form.⁵⁶ A stable cyclic nitrogen pentasulfide 2,6-Mes₂-4-MeC₆H₂NS₅ (**62**, Figure 6) was produced by passing the *N*-thiosulfinylaniline 2,6-Mes₂-4-MeC₆H₂NS₂ (**63**) through a silica column,⁵⁷ along with the sulfur diimide (2,6-Mes₂-4-MeC₆H₂N)₂S (**64**), as a minor product. The mechanism of the formation of **62** was not clear, but it is conceivable that it proceeds *via* the trimerisation of **63**, which could eliminate the diimide with concomitant formation of the pentasulfide. In **62** the NS₅ ring adopts a chair conformation and the nitrogen atom adopts an almost planar geometry.

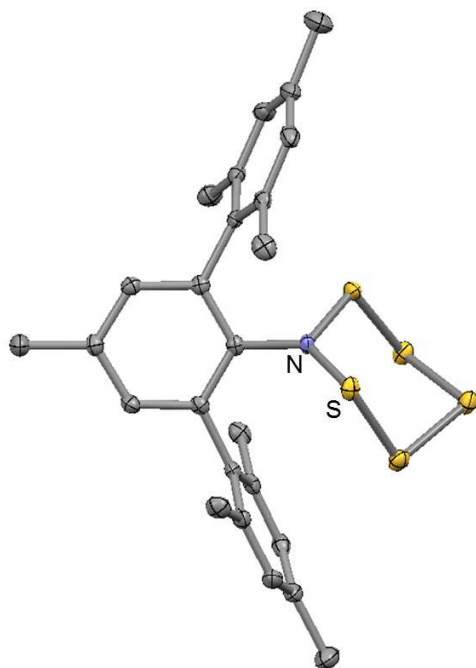


Figure 6 The molecular structure of 2,6-Mes₂-4-MeC₆H₂NS₅ (**62**) with thermal ellipsoids set at 50%.⁵⁷ Hydrogen atoms are omitted for clarity.

3. Carbazol-9-yl Ligands Featuring Sterically Demanding Substituents

Carbazoles are aromatic, heterocyclic compounds which consist of two benzene rings fused opposite each other on a five-membered pyrrole ring (Figure 7). This provides a rigid structure which is excellent for the introduction of functionality in particular into the 1 and 8-positions in order to increase the steric bulk around a nitrogen-coordinated element. In terms of the central nitrogen ring, there are differing modes of coordination available within carbazol-9-yl complexes – the extremes of which can be seen in Figure 7; the ligand can act as a classic monodentate, amide σ -donor or it can act as a multihapto ligand, forming a π -complex. It is also possible to coordinate to the fused benzene rings, as has been observed in the structure of the caesium compound of the parent carbazol-9-yl ligand as determined by powder X-ray diffraction.⁵⁸

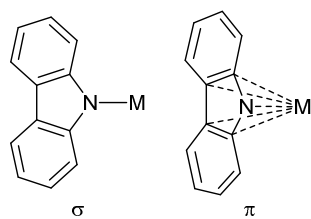


Figure 7 Schematic representation of monohapto (left) and multihapto (right) bonding modes of carbazol-9-yl ligands.

Substituted carbazol-9-yl ligands are finding use in transition metal and lanthanide chemistry, affording compounds with potential applications such as fluorescent probes for anion detection⁵⁹ and in the catalysis of a range of reactions.⁶⁰⁻⁶³ A number of these complexes utilise intramolecular donors on the carbazolyl ligand framework, but we will only consider the monodentate carbazolyl ligands which feature sterically demanding substituents in order to stabilise low-coordinate and highly reactive main group centres. Attention will be focussed on two classes of 1,8-substituted carbazolyl ligands: 1,3,6,8-tetra-*tert*-butylcarbazolyl and 1,8-diarylcarbazolyl ligands (Figure 8). Due to their similarity in terms of steric demands, the 1,8-diarylcarbazolyls have been proposed as competitors to *m*-terphenyl ligands, potentially offering a higher degree of steric protection than these aryl counterparts.⁶⁴

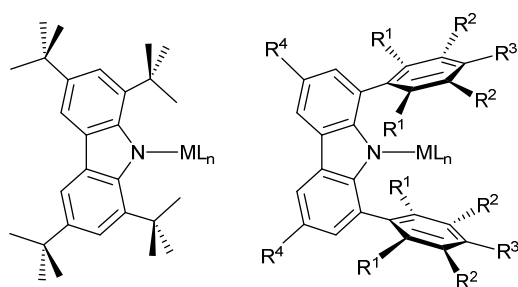
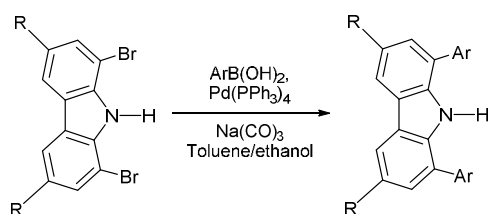


Figure 8 1,3,6,8-tetra-*tert*-butylcarbazolyl (left) and 1,8-diarylcarbazolyl ligands (right).

1,3,6,8-Tetra-*tert*-butylcarbazole (1,3,6,8-*t*Bu₄carbH) was first synthesised in order to stabilise a monomeric aminyl radical, which has the unpaired electron largely delocalised over

the planar π -system.⁶⁵ 1,3,6,8-tetra-*tert*-butylcarbazole is synthesised through the Friedel-Crafts reaction between carbazole and excess *tert*-butyl chloride in the presence of an AlCl_3 catalyst. The 1,8-diarylcarbazolyl ligand precursors (1,8- Ar_2 -3,6- R_2 carbH; Ar = aryl, R = Me, *t*Bu) are synthesised through the Suzuki cross-coupling reactions between the 1,8-dibromo-3,6-dialkylcarbazole and an arylboronic acid using a $\text{Pd}(\text{PPh}_3)_4$ catalyst (Scheme 4).⁶⁶ An advantage of these 1,8-diarylcarbazolyls is the potential for altering the steric and electronic properties of the ligands through the variation of the aryl substituents, although it has been proposed that there are limits to the size of these flanking aryls.⁶⁴



Scheme 4 The synthesis of 1,8-diarylcarbazolyl ligand precursors (1,8- Ar_2 -3,6- R_2 carbH, Ar = aryl substituent, R = Me, *t*Bu).

3.1 s-Block Complexes

The 1,3,6,8-tetra-*tert*-butylcarbazolyl lithium salts have been isolated as DME (DME = 1,2-dimethoxyethane) and THF adducts which exist as solvent separated ion pairs in the solid state; $[\text{Li}(\text{DME})_3][1,3,6,8\text{-}^t\text{Bu}_4\text{carb}]$ (**65**) and $[\text{Li}(\text{THF})_4][1,3,6,8\text{-}^t\text{Bu}_4\text{carb}]$ (**66**).⁶⁷ Conversely, $1,3,6,8\text{-}^t\text{Bu}_4\text{carbLi}(\text{THF})_2$ (**67**), when crystallised from a hexane/THF mixture, exists in a solvated structure in the solid state.⁶⁸ Unsolvated $[1,3,6,8\text{-}^t\text{Bu}_4\text{carbLi}]_2$ (**68**) forms as an amide-bridged dimer in the solid state, featuring η^1 - and η^5 -carbazolyl interactions (Figure 9).^{68,69} This type of interaction which features simultaneous σ -donation to one lithium centre and π -donation to the other lithium had been predicted previously by MNDO and *ab initio* calculations for the related *N*-lithiopyrrole,⁷⁰ but had not been observed in an isolated species until the report of **68**. In addition to **67**, the analogous sodium and potassium salts,

1,3,6,8-*t*Bu₄carbNa(THF)₃ (**69**, Figure 9) and 1,3,6,8-*t*Bu₄carbK(THF)₄ (**70**) bind three and four THF molecules, respectively, concomitant with increasing cation size.⁶⁸ In the solid state structures of these complexes there is an increase in the hapticity of the binding of the carbazol-9-yl ligands upon descending Group 1, mirroring the increasing ionic bonding character. Associated with this can be seen the increasingly acute centroid–N–M angle on moving from **67** [111.56(2)°] to **69** [102.23(2)°] to **70** [80.51(2)°].

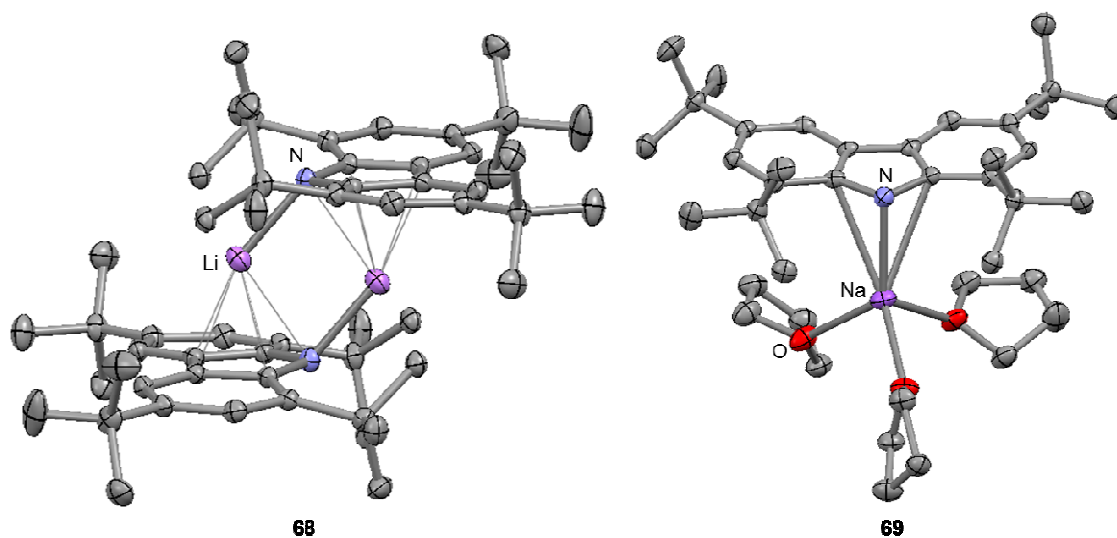


Figure 9 The molecular structures of [1,3,6,8-*t*Bu₄carbLi]₂ (**68**) and 1,3,6,8-*t*Bu₄carbNa(THF)₃ (**69**) with thermal ellipsoids set at 50%.⁶⁸ Hydrogen atoms are omitted for clarity.

The lithium species 1,8-Ar₂-3,6-Me₂carbLi (Ar = Ph **71**, Mes **72**) have been utilised in the synthesis of main group and transition metal complexes *via* salt metathesis reactions.^{64,66,71} The potassium salt [(1,8-Ph₂-3,6-Me₂carb)K]₂ (**73**) was isolated in low yield as a by-product from the potassium reduction of (1,8-Ph₂-3,6-Me₂carb)GaCl₂ (**74**).⁶⁴ The solid state structure of **73** exhibits a K–N bond [2.745(2) Å] as well as potassium-arene interactions to both the carbazolyl and phenyl rings. The potassium is significantly deviated from the carbazolyl ligand plane [centroid–N–K angle = 150.37(5)°]. The 3,5-xylyl- and mesityl-

substituted compounds $[(1,8\text{-Ar}_2\text{-}3,6\text{-}^t\text{Bu}_2\text{carb})\text{K}(\text{THF})_n]_m$ (Ar = Xyl, $n = 1$, $m = 2$ **75**; Ar = Mes, $n = 2$, $m = 1$ **76**) have been synthesised *via* the reaction between the carbazole and KH in THF solution.⁷² Like **73**, the crystal structure of **75** is also a dimer, but the K^+ ions are bound to the pyrrolyl nitrogen of one carbazolyl unit [$\text{K}\text{-N}$ distance = 2.758(3) Å] and through an η^6 -arene interaction with one of the condensed six-membered rings of the other carbazolyl ligand, along with long-range interactions to the flanking xylyl substituents; a mix of hard and soft coordination modes.

1,3,6,8- $^t\text{Bu}_4\text{carbMgEt}(\text{THF})_2$ (**77**), synthesised *via* the reaction between 1,3,6,8-tetra-*tert*-butylcarbazole and diethyl magnesium, features a four-coordinate magnesium centre which is distorted from the plane of the carbazolyl ligand by 117.4°.⁷³ Subsequently, the Hauser bases 1,3,6,8- $^t\text{Bu}_4\text{carbMgI}(\text{THF})_2$ (**78**) and 1,8- $\text{Ar}_2\text{-}3,6\text{-}^t\text{Bu}_2\text{carbMgI}(\text{THF})$ (Ar = Xyl **79**, Mes **80**) have been synthesised *via* the reaction between **70**, **75** or **76** and MgI_2 .⁷² Whilst **78** features a four-coordinate magnesium cation with the coordination of the metal centre in a pseudo- π interaction (Figure 10), much like the ethyl analogue,⁷³ the solid state structure of **80** features a formally three-coordinate magnesium centre (Figure 10). This is a rare coordination environment for magnesium, and is stabilised by the steric pocket created by the flanking mesityl substituents of the carbazolyl ligand.

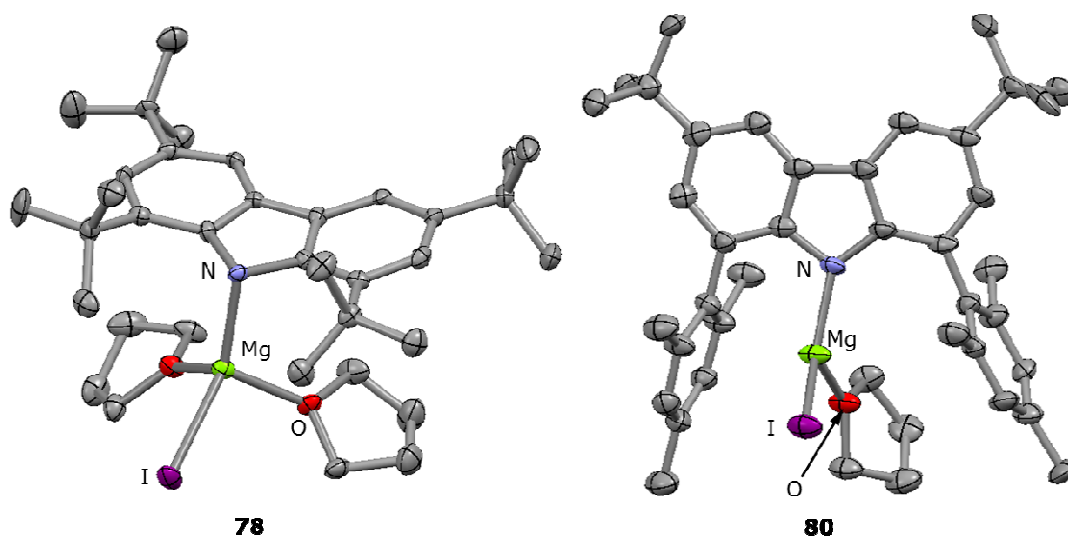


Figure 10 The molecular structures of 1,3,6,8-*t*Bu₄carbMgI(THF)₂ (**78**) and 1,8-Mes₂-3,6-*t*Bu₂carbMgI(THF) (**80**) with thermal ellipsoids set at 50%.⁷² Hydrogen atoms are omitted for clarity.

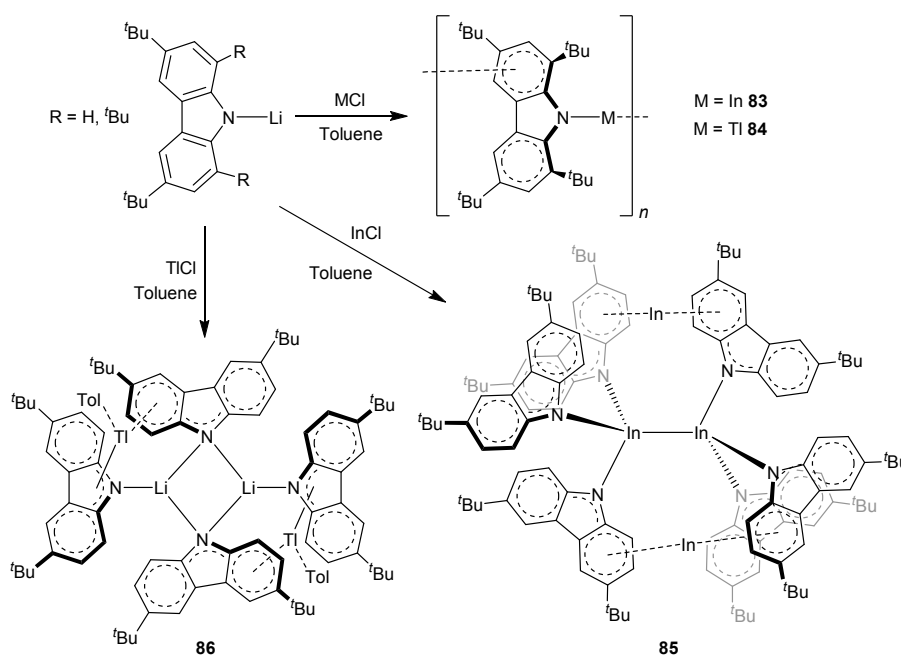
Comparison of the potassium and magnesium carbazol-9-yl compounds reveals significant differences in the coordination modes which are dependent on the nature of the 1- and 8-substituents: ligands with *tert*-butyl substituents in the 1- and 8 positions afford π -type compounds, in which the carbazolyl ligand acts more as a multihapto donor, whereas ligands with 1,8-diaryl substituents yield σ -type compounds. Percent buried volume calculations (%V_{Bur}) have been used to quantify the steric demands of the ligands in these compounds; this was calculated to be 51.9% for **78** and 54.7% for **80**.

The homoleptic calcium *bis*(carbazolyl) (1,3,6,8-*t*Bu₄carb)₂Ca (**81**) was synthesised through the reaction between (C₁₀H₈)Ca(THF)₂ and two equivalents of 1,3,6,8-*t*Bu₄carbH.⁷⁴ As has been seen for the related cadmium complex (1,3,6,8-*t*Bu₄carb)₂Cd (**82**),⁶⁹ in **81** the two carbazolyl ligands lie parallel, but are rotated 180° away from each other. The calcium atoms are not central underneath the carbazolyl five-membered ring, but are oriented towards the azaallyl moiety.

3.2 Group 13 Complexes

tert-Butyl-substituted carbazolyl ligands have been used to stabilise Group 13 M(I) complexes, the tuning of the *tert*-butyl groups in the 1- and 8-positions affording complexes with different ligand binding modes (Scheme 5).⁶⁷ The salt metathesis reaction between the 1,3,6,8-*t*Bu₄carb⁻ ligand and indium(I) or thallium(I) chloride affords the isostructural carbazolyl complexes 1,3,6,8-*t*Bu₄carbIn (**83**) and 1,3,6,8-*t*Bu₄carbTl (**84**), in which the metal is η^3 -bound to the central pyrrolyl ring of the ligand, and adopts a one-dimensional

coordination polymer through additional secondary η^6 -arene interactions to an adjacent carbazolyl ligand. Metathesis reactions between the less bulky 3,6- t Bu₂carb⁻ ligand and indium(I) or thallium(I) chloride afford the mixed valence product In₂[In(3,6- t Bu₂carb)₆] (**85**) for the more redox active indium and the mixed lithium/thallium amide [Ti(toluene)]₂[Li₂(3,6- t Bu₂carb)₄] (**86**), indicating that the less bulky carbazolyl ligand 3,6- t Bu₂carb⁻ functions more readily as a σ -donor.



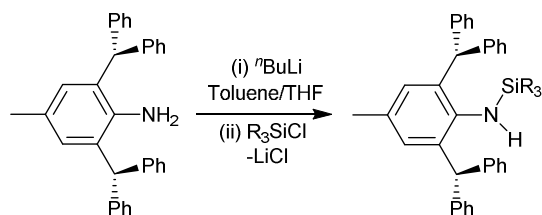
Scheme 5 The synthesis of complexes **83-86** highlighting bonding flexibility depending on substituents in the 1- and 8-positions.⁶⁷

Dialkylaluminium complexes 1,8-Ph₂-3,6-Me₂carbAlR₂ (R = Me **87**, Et **88**) have been investigated for their propensity to form cationic aluminium complexes.⁶⁶ Treatment of the complexes with B(C₆F₅)₃ or [H(OEt₂)₂][B{3,5-(CF₃)₂C₆H₃}₄] affords [1,8-Ph₂-3,6-Me₂carbAlR]⁺ (R = Me **89**, Et **90**) species, which subsequently form alkyl/aryl exchange products. The cationic species show a low activity for the oligomerisation of ethylene, yielding low molecular weight (C₄-C₁₀) olefinic products.

Gallium complexes 1,8-Ar₂-3,6-Me₂carbGaCl₂ (Ar = Ph **74** Mes **91**) have been synthesised from the reaction between lithium salts **71** or **72** and GaCl₃.⁶⁴ While samples of **74** were deemed to be unlikely to be compatible with the isolation of low-coordinate gallium systems due to a high degree of conformational flexibility, the bulkier mesityl-substituted ligand afforded **91**, which was the first example of a monomeric, three-coordinate gallium dihalide. Comparison of the Tolman cone angles for 1,8-Mes₂-3,6-Me₂carb⁻ ($\theta = 269^\circ$) with the *m*-terphenyls 2,6-Ar₂C₆H₃⁻ (Ar = Mes, $\theta = 185^\circ$; Ar = Trip, $\theta = 201^\circ$) highlight the greater steric protection of the 1,8-diarylcarbazolyl ligand compared to their *m*-terphenyl analogues.

4. Amide ligands based on bulky anilines with C₆H₂{C(H)Ph₂}₂R-2,6,4 (R = alkyl)

The facile synthesis of the highly bulky primary aniline Ar^{*}NH₂ (Ar^{*} = C₆H₂{C(H)Ph₂}₂Me-2,6,4) was reported in 2010 by Berthon-Gelloz, Markó and co-workers, who used it in the preparation of an *N*-heterocyclic carbene :C{N(Ar^{*})C(H)}₂.⁷⁵ Jones *et al.* reasoned that this primary amine would be an excellent precursor for the synthesis of extremely bulky secondary amines of the type Ar^{*}N(H)SiR₃ (Scheme 6; R₃ = Me₃, MePh₂, Ph₃),⁷⁶ which can be used as proligands for the stabilisation of main group and transition metal complexes. This chemistry has been expanded to incorporate other aryl and silyl groups, allowing a high degree of tuning of the ligand steric demands, and therefore the resulting complexes of these ligands. The bulky *bis*(aryl)amines, (Ar^{*})N(H)Ar [Ar = Ph, Mes, C₆H₃-3,5-(CF₃)₂, Trip], can be prepared *via* palladium-catalysed cross-coupling reactions.^{77,78}



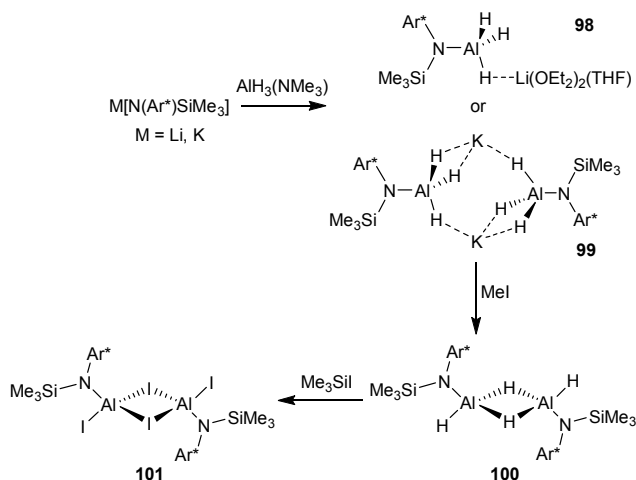
Scheme 6 The synthesis of Ar^{*}N(H)SiR₃ (R₃ = Me₃, MePh₂, Ph₃) ligand precursors.⁷⁶

4.1 s-Block Complexes

As with other amide ligands, the development of alkali metal salts is extremely useful in their utilisation in the synthesis of new main group compounds through metathesis chemistry. The secondary amines $\text{Ar}^*\text{N}(\text{H})\text{SiR}_3$ are readily deprotonated using $^n\text{BuLi}$, NaH or KH in ethereal solvents, with the crystal structures of $[\text{Li}\{\text{N}(\text{Ar}^*)\text{SiMe}_3\}(\text{L})]$ ($\text{L} = \text{OEt}_2$ **92** or THF **93**), $\text{Na}\{\text{N}(\text{Ar}^*)\text{SiMe}_3\}(\text{THF})_3$ (**94**) and $\text{K}\{\text{N}(\text{Ar}^*)(\text{SiPh}_3)\}(\text{OEt}_2)$ (**95**) showing that they are monomeric in the solid state.⁷⁶ The potassium salt of the highly encumbered ligand $[\text{N}(\text{Ar}^\dagger)\text{Si}^i\text{Pr}_3]^-$ ($\text{Ar}^\dagger = \text{C}_6\text{H}_2\{\text{C}(\text{H})\text{Ph}_2\}_2^i\text{Pr}-2,6,4$) has been structurally authenticated as the toluene adduct $\text{K}\{\text{N}(\text{Ar}^\dagger)\text{Si}^i\text{Pr}_3\}(\eta^6\text{-toluene})$ (**96**).⁷⁹ This ligand has been used in the synthesis of dimeric $[\text{Mn}(\mu\text{-Br})\{\text{N}(\text{Ar}^\dagger)\text{Si}^i\text{Pr}_3\}]_2$, which forms the highly unusual two-coordinate, high-spin manganese(0) complex $\{\text{Ar}^\dagger\text{NSi}^i\text{Pr}_3\}\text{MnMg}(\text{MesNacnac})$ ($\text{MesNacnac} = [(\text{MesNCMe})_2\text{CH}]^-$), featuring an unsupported Mn–Mg bond.⁸⁰

4.2 Group 13 Complexes

Attempts to utilise the $[\text{N}(\text{Ar}^*)\text{SiMe}_3]^-$ ligand to stabilise an Al(I) species, through reaction between the Li or K salts and metastable $[\text{AlCl}(\text{THF})]_n$ did not yield any reaction products.⁸¹ Similarly, there was no salt elimination reaction between **96** and $[\text{AlCl}(\text{THF})]_n$.⁷⁹ This lack of reactivity contrasts with that of the heavier congeners (see below). The preparation of aluminium(III) halide complexes has been reported. Whilst the bromide complex $\text{Me}_3\text{Si}(\text{Ar}^*)\text{NAlBr}_2(\text{THF})$ (**97**) could be synthesised *via* the salt metathesis reaction, an analogous reaction with AlI_3 yielded only an intractable mixture of products. Aluminium hydride precursor complexes **98-100**, of significant interest in their own right, were synthesised and converted to $[\text{Me}_3\text{Si}(\text{Ar}^*)\text{NAlI}_2]_2$ (**101**) (Scheme 7). All efforts to reduce these complexes to Al(I) systems with a variety of reducing agents met without success.



Scheme 7 The synthesis of aluminium(III) complexes **98-101**.⁸¹

The reaction between **96** and the Group 13 tribromides BBr_3 or $AlBr_3$ did not yield the corresponding complexes ${}^iPr_3Si(Ar^\dagger)NEBr_2$ ($E = B, Al$), but instead affords the hydrido-bromoborane ${}^iPr_3Si(Ar^\dagger)NB(H)Br$ (**102**) and an aluminacycle $AlBr_2\{\kappa^2-C,N-N(H)(Si^iPr_3)\{C_6H_2[CPH_2][C(H)Ph_2]^iPr-2,6,4\}\}$ (**103**, Figure 11), respectively.⁷⁹ It is postulated that **103** is formed *via* the intramolecular migration of one of the benzhydryl methine protons on the $[N(Ar^\dagger)Si^iPr_3]^-$ ligand to the nitrogen, with concomitant aluminium of the methine carbon atom. Intramolecular interactions as seen in the structure of potassium complex **96** could facilitate an intramolecular C–H activation of the likely reaction intermediate ${}^iPr_3Si(Ar^\dagger)NAlBr_2$. No similar migration chemistry was observed in the methyl-substituted analogue **97**,⁸¹ which may be due to the coordination of the THF molecule to the aluminium centre reducing the Lewis acidity of this site. A similar mechanism may also proceed to form borane **102**. Attempted reductions of these compounds were unsuccessful.

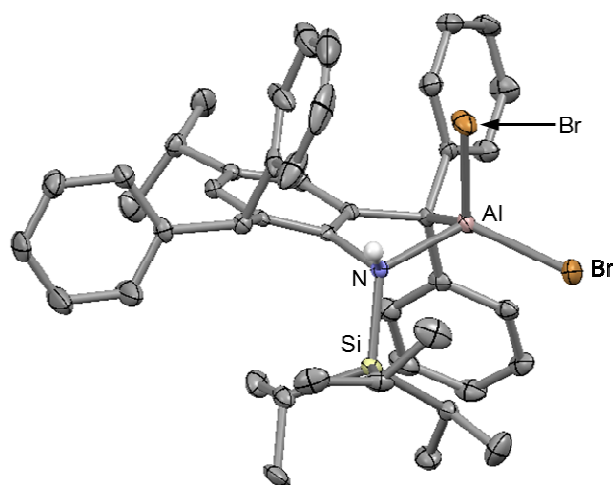


Figure 11 The molecular structure of $\text{AlBr}_2\{\kappa^2\text{-C,N-N(H)(Si}^i\text{Pr}_3\}\{\text{C}_6\text{H}_2[\text{CPh}_2][\text{C(H)Ph}_2]^i\text{Pr-2,6,4}\}$ (**103**) with thermal ellipsoids set at 50%. Hydrogen atoms, with the exception of the nitrogen-bound hydrogen are omitted for clarity.⁷⁹

Although the Al(I) complexes could not be prepared, the $[\text{N}(\text{Ar}^*)\text{SiR}_3]^-$ ligand has yielded a series of monomeric, heavier Group 13 metal(I) amide complexes $\text{MN}(\text{Ar}^*)\text{SiMe}_3$ ($\text{M} = \text{Ga}$ **104**, In **105**, Tl **106**) and $\text{MN}(\text{Ar}^*)\text{SiPh}_3$ ($\text{M} = \text{Ga}$ **107** Figure 12, Tl **108**).⁸¹ These complexes were prepared *via* the metathesis reactions between the ligand alkali metal salts and MX ($\text{X} = \text{Cl}, \text{Br}$). Structural and computational investigations reveal that the metal centres are truly one-coordinate, and do not exhibit any significant intra- or intermolecular interactions in addition to the N–M bond. Calculations also show that the gallium lone pair has essentially *s*-character. Metal(I) complexes **104** and **105** have provided access to remarkable *bis*(boryl) complexes which are the first thermally stable, monomeric Ga(II)X_2 and In(II)X_2 radicals.⁸²

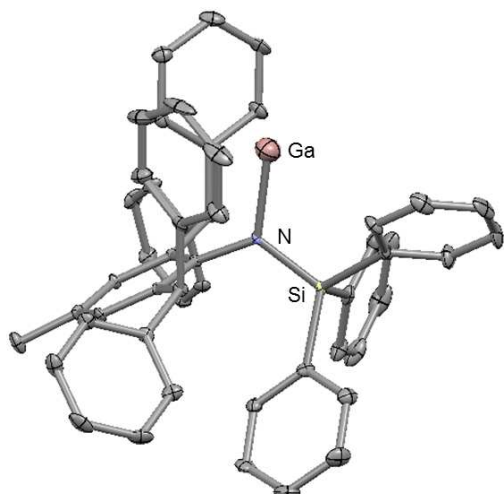


Figure 12 The molecular structure of $\text{GaN}(\text{Ar}^*)\text{SiPh}_3$ (**107**), with thermal ellipsoids set at 50% and hydrogen atoms omitted for clarity.⁸¹

4.3 Group 14 Complexes

4.3.1 Element (IV) Complexes

The Si(IV) complexes $\text{R}_3\text{Si}(\text{Ar}^*)\text{NSi}(\text{X})\text{Cl}_2$ ($\text{R} = \text{Me}_3$, $\text{X} = \text{Cl}$ **109**; $\text{R} = \text{MePh}_2$, $\text{X} = \text{Cl}$ **110**; $\text{R} = \text{Ph}_3$, $\text{X} = \text{Cl}$ **111**; $\text{R} = \text{Me}_3$, $\text{X} = \text{H}$ **112**) were synthesised *via* the metathesis reactions between the lithium complexes and $\text{Si}(\text{X})\text{Cl}_3$.⁷⁶ The solid state structures of these compounds feature two distorted tetrahedral silicon centres, with SiNSi moieties which are essentially orthogonal to the anilide moiety, as has been observed in the related $\text{Me}_3\text{Si}(\text{Dipp})\text{NSiMeCl}_2$.⁸³

4.3.2 Element-Element Bonds

These ligands have been used to stabilise low nuclearity/low oxidation state Group 14 compounds in analogy to the *m*-terphenyl complexes reported by Power.^{26f,26g,84} $\text{Me}_3\text{Si}(\text{Ar}^*)\text{NGe}(\text{Cl})$ (**113**) is reduced using half an equivalent of the magnesium(I) dimer $[(^{\text{Mes}}\text{Nacnac})\text{Mg}]_2$ to yield $\text{Me}_3\text{Si}(\text{Ar}^*)\text{NGeGeN}(\text{Ar}^*)\text{SiMe}_3$ (**114**, Figure 13), which is remarkable as the first digermene with a Ge–Ge single bond.⁸⁵ The solid state structure of **114**

reveals a *trans*-bent dimer structure with acute N–Ge–Ge angles of $100.09(6)^\circ$ and a long Ge–Ge distance [$2.7093(7) \text{ \AA}$], which is over 0.4 \AA longer than found in multiply bonded digermynes.^{26f,26g,86} The near coplanar arrangement of the NSiCGe and Ge₂N₂ units prevents Ge–Ge multiple bonding, and DFT calculations show the Ge–Ge single bond possesses considerable *p*-character (92.8%).

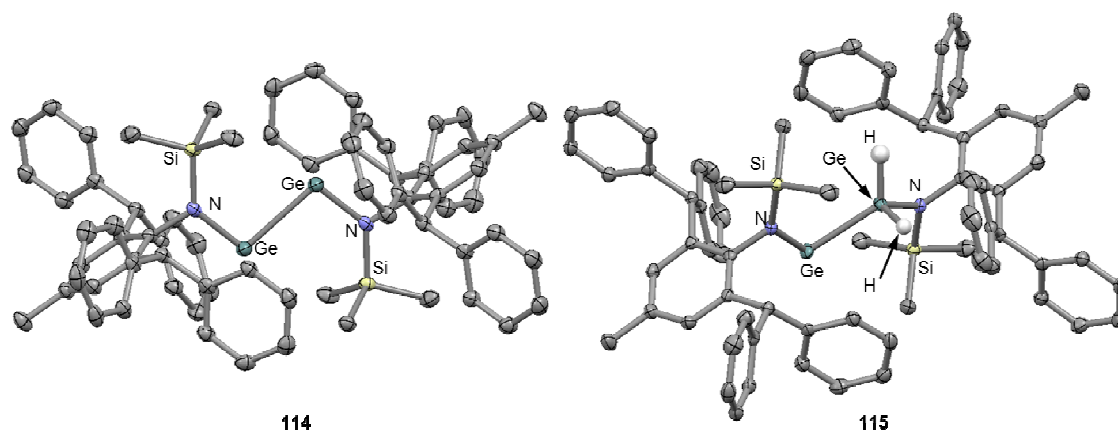
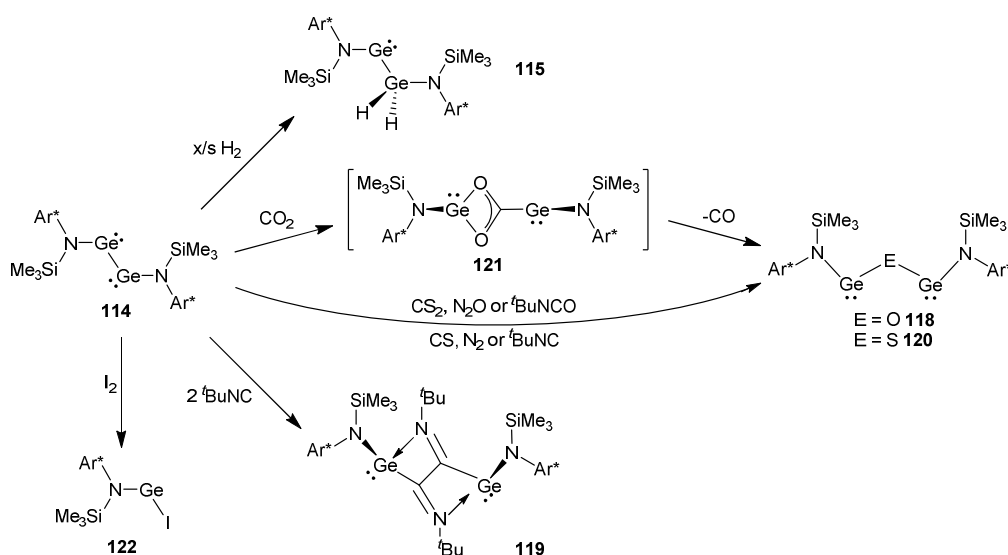


Figure 13 The molecular structures of $\text{Me}_3\text{Si}(\text{Ar}^*)\text{NGeGeN}(\text{Ar}^*)\text{SiMe}_3$ (**114**) and $\text{Me}_3\text{Si}(\text{Ar}^*)\text{NGeGe}(\text{H})_2\text{N}(\text{Ar}^*)\text{SiMe}_3$ (**115**) with thermal ellipsoids set at 50%.⁸⁵ Hydrogens, with the exception of the germanium-bound hydrides in **115** are omitted for clarity.

114 cleanly activates dihydrogen both in solution and in solid state reactions at room temperature, yielding $\text{Me}_3\text{Si}(\text{Ar}^*)\text{NGeGe}(\text{H})_2\text{N}(\text{Ar}^*)\text{SiMe}_3$ (**115**, Figure 13 and Scheme 8),⁸⁵ where two hydrogen atoms have added to one of the germanium centres. The formal double hydrogenation product, $\text{Me}_3\text{Si}(\text{Ar}^*)\text{N}(\text{H}_2)\text{GeGe}(\text{H}_2)\text{N}(\text{Ar}^*)\text{SiMe}_3$ (**116**), could not be formed from the reaction between **115** and further equivalents of dihydrogen, even at elevated temperatures. Computational calculations show that the barrier to this second hydrogenation is kinetic in nature. Mixtures of **115** and **116** could be obtained through the reaction between **113** and $\text{Li}[\text{HB}^t\text{Bu}_3]$ or $\text{K}[\text{HBET}_3]$. It has been proposed that **115** exists in equilibrium with the symmetrical Ge(II) isomer $\text{Me}_3\text{Si}(\text{Ar}^*)\text{N}(\text{H})\text{GeGe}(\text{H})\text{N}(\text{Ar}^*)\text{SiMe}_3$ (**117**) in solution.

DFT calculations have shown that the hydrogenation reaction is stepwise: the addition of the first molecule of H₂ affords a singly bridged species Me₃Si(Ar*)N(H)Ge(μ-H)GeN(Ar*)SiMe₃, which then rearranges to **117** and the experimentally observed isomer **115**.^{87,88} Calculations on model complexes suggest that the reactivity of the amide-substituted ditetrylynes has the order Si > Ge > Sn, and that the Sn–Sn system forms the symmetrically-bridged hydride upon reaction with dihydrogen, which has been observed experimentally (see below).^{87,88}



Scheme 8 The small molecule reactivity of Me₃Si(Ar*)N-Ge-Ge-N(Ar*)SiMe₃ (**114**).^{78,85,89}

114 quantitatively reduces CO₂ to CO, yielding the *bis*(germylene) oxide [Me₃Si(Ar*)N-Ge]₂O (**118**) as the by-product (Scheme 8).⁸⁹ This reaction is significant as it is almost unprecedented for the p-block elements, and this was the first example of the generation of CO from CO₂ by germanium. Spectroscopic and computational investigations show that this reaction likely proceeds through an unsymmetrically-bound intermediate Me₃Si(Ar*)N-Ge(η²-CO₂)-GeN(Ar*)SiMe₃ (**121**). Compound **118** could also be formed from the reactions between **114** and N₂O or ^tBuNCO. In the N₂O reaction, no further oxidation of the Ge(II) centres was observed, which is in contrast to the analogous *m*-terphenyl complex.⁹⁰

For the t BuNCO reaction the by-product t BuNC was not observed, but is rapidly consumed yielding the reductively coupled product $[\text{Me}_3\text{Si}(\text{Ar}^*)\text{NGeC}=\text{N}^t\text{Bu}]_2$ (**119**). **114** also reduces CS_2 to CS yielding the *bis*(germylene) sulfide $[\text{Me}_3\text{Si}(\text{Ar}^*)\text{NGe}]_2\text{S}$ (**120**). The reaction between **114** and one equivalent of I_2 affords the germanium(II) iodide $\text{Me}_3\text{Si}(\text{Ar}^*)\text{NGe}(\text{I})$ (**122**) *via* the oxidative cleavage of the Ge–Ge bond.⁷⁸

Remarkably, increasing the steric bulk of the amide ligand does not lead to the formation of the monomeric species, but instead yields ${}^i\text{Pr}_3\text{Si}(\text{Ar}^\dagger)\text{NGeGeN}(\text{Ar}^\dagger)\text{Si}^i\text{Pr}_3$ (**123**), which unlike **114** features a Ge–Ge multiple bond.⁹¹ The UV/visible spectrum for **114** displays absorption bands at $\lambda_{\text{max}} = 531$ nm and 383 nm,⁸⁵ whilst **123** exhibits two absorption bands at $\lambda_{\text{max}} = 399$ nm and 472 nm,⁹¹ which are similar to the $\pi \rightarrow \pi^*$ and $n_- \rightarrow n_+$ transitions for multiply bonded digermynes, indicating a significant electronic difference between these systems. The Ge–Ge distance for **123** is 2.3568(3) Å – more than 0.35 Å shorter than that in **114**. The greater steric bulk of the $[\text{}^i\text{Pr}_3\text{Si}(\text{Ar}^\dagger)\text{N}]^-$ ligand prevents the planarisation of the Ge_2NSiC fragments in **123** which disallows $\text{N} \rightarrow \text{Ge}$ π -bonding. DFT calculations show that the HOMO for **123** is a π -bond orthogonal to the Ge_2N_2 fragment, while the essentially non-bonding HOMO–1, a “slipped” π -orbital is thought to give rise to singlet biradicaloid character. For **123** the calculated Wiberg Bond Index (WBI) value of 1.75 contrasts with a WBI of 0.94 for **114**. The isolation of complexes **114** and **123** show that by utilising these bulky $[\text{R}_3\text{Si}(\text{R})\text{N}]^-$ ligands steric control over the Ge–Ge bond orders can be exerted.

123 activates dihydrogen below 0 °C affording the symmetrical hydride ${}^i\text{Pr}_3\text{Si}(\text{Ar}^\dagger)\text{N}(\text{H})\text{GeGe}(\text{H})\text{N}(\text{Ar}^\dagger)\text{Si}^i\text{Pr}_3$ (**124**, Figure 14), which features a long Ge=Ge double bond [2.4864(4) Å],⁹¹ significantly longer than for the *m*-terphenyl analogue 2,6-Dipp₂C₆H₃(H)Ge=Ge(H)C₆H₃Dipp_{2-2,6} [2.3026(3) Å].⁹² **124** was postulated to exist in equilibrium with the hydrido-germylene ${}^i\text{Pr}_3\text{Si}(\text{Ar}^\dagger)\text{NGe}(\text{H})$ (**125**) in solution, with spectroscopic studies and the isolation of the 4-dimethylaminopyridine (DMAP) adduct

$i\text{Pr}_3\text{Si}(\text{Ar}^\dagger)\text{NGe}(\text{H})(\text{DMAP})$ (**126**, Figure 14) providing some evidence to support this. **124** can also be synthesised through the reaction between $i\text{Pr}_3\text{Si}(\text{Ar}^\dagger)\text{NGe}(\text{Cl})$ (**127**) and $\text{Li}[\text{HB}^i\text{Bu}_3]$. The tin analogue could not be formed through this method, as the reaction between $i\text{Pr}_3\text{Si}(\text{Ar}^\dagger)\text{NSn}(\text{Cl})$ (**128**) and $\text{Li}[\text{HB}^i\text{Bu}_3]$ yielded the hydride-bridged dimer $[i\text{Pr}_3\text{Si}(\text{Ar}^\dagger)\text{NSn}(\mu\text{-H})]_2$ (**129**). This complex dissociates in solution, and forms the adduct $i\text{Pr}_3\text{Si}(\text{Ar}^\dagger)\text{NSn}(\text{H})(\text{DMAP})$ (**130**) with added DMAP.

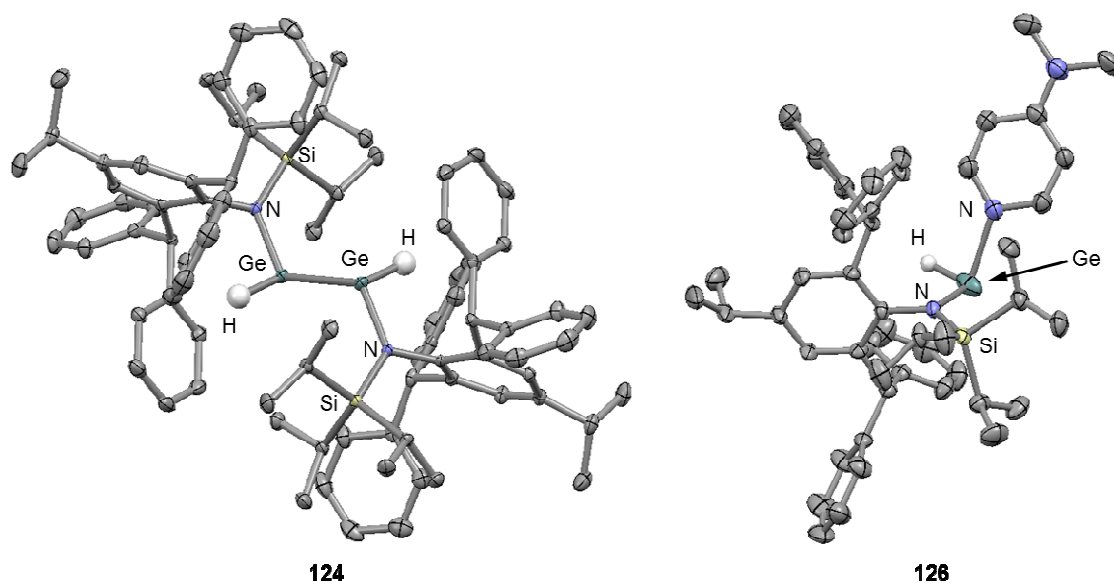


Figure 14 The molecular structures of $i\text{Pr}_3\text{Si}(\text{Ar}^\dagger)\text{N}(\text{H})\text{GeGe}(\text{H})\text{N}(\text{Ar}^\dagger)\text{Si}^i\text{Pr}_3$ (**124**) and $i\text{Pr}_3\text{Si}(\text{Ar}^\dagger)\text{NGe}(\text{H})(\text{DMAP})$ (**126**), with thermal ellipsoids set at 50%.⁹¹ Hydrogen atoms, with the exception of the germanium-bound hydrides, are omitted for clarity.

In contrast to the germanium analogue **123**, the distannyne complex $i\text{Pr}_3\text{Si}(\text{Ar}^\dagger)\text{NSnSnN}(\text{Ar}^\dagger)\text{Si}^i\text{Pr}_3$ (**131**) features a long Sn–Sn single bond [3.1429(7) Å, ave. N–Sn–Sn angle = 104.00°].⁹³ The larger tin radius allows the adoption of planar Sn_2NSiC moieties allowing a degree of $\text{N} \rightarrow \text{Sn}$ π -donation, despite the significant steric demands of the $[i\text{Pr}_3\text{Si}(\text{Ar}^\dagger)\text{N}]^-$ ligands. The reaction between **131** and dihydrogen afforded the hydride-bridged dimer **129**.⁹¹ This hydrogenation proceeded much slower than that for the germanium

analogue and a different isomer of the hydrogenation product was obtained, which was predicted by theory.⁸⁷ The hydrogenation of **131** to **129** has been calculated to be essentially thermo-neutral, and thus may be reversible under mild conditions, but this has not been observed experimentally.⁹³ The reaction between **131** and ^tBuNC affords the adduct ^tPr₃Si(Ar[†])N(^tBuNC)SnSn(^tBuNC)N(Ar[†])Si^tPr₃ (**132**, Figure 15), which unlike the *m*-terphenyl analogue⁹⁴ does not show any dissociation of the isocyanide in solution under ambient conditions.

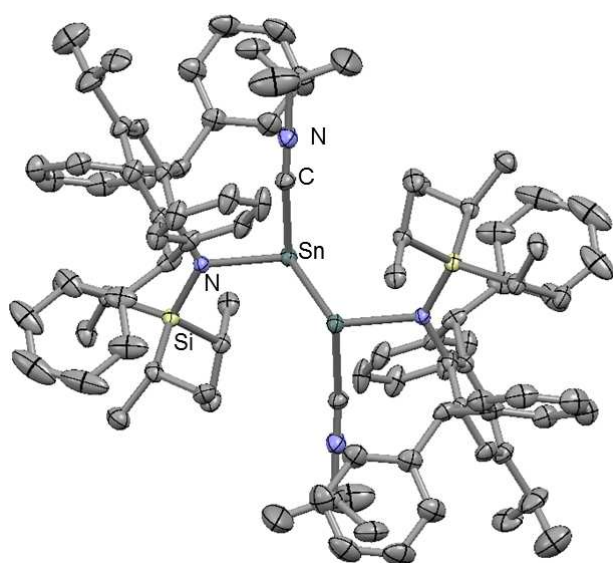


Figure 15 The molecular structure of ^tPr₃Si(Ar[†])N(^tBuNC)SnSn(^tBuNC)N(Ar[†])Si^tPr₃ (**132**), with thermal ellipsoids set at 50%.⁹³ Hydrogen atoms are omitted for clarity.

4.3.3 Monomeric Element(II) Derivatives

The germanium and tin complexes R₃Si(Ar^{*})NM(Cl) (M = Ge, R₃ = Me₃ **113**, MePh₂ **133**, Ph₃ **134**; M = Sn, R₃ = Me₃ **135**, MePh₂ **136**, Ph₃ **137**) are monomeric, whilst the Pb(II) derivatives are chloride-bridged dimers [R₃Si(Ar^{*})NPb(μ-Cl)]₂ (R₃ = Me₃ **138**, MePh₂ **139**) in the solid state.⁷⁶ The Ge and Sn complexes **113**, **135** and **137** were the first structurally authenticated monomeric, two-coordinate amide Group 14 complexes featuring a halide; the

closest analogues in the literature being stabilised by *m*-terphenyl ligands.⁹⁵ The N–E–Cl angles of 98.85(9)°, 96.49(10)° and 98.10(7)° for **113**, **135** and **137**, respectively, which imply significant *s*-character in the lone pairs on the metals. This chemistry has been extended to the silyl complexes Me₃Si(Ar[†])NGe(Cl) (**140**) and Me₃Si(Ar^{tBu})NGe(Cl) (**141**, Ar^{tBu} = C₆H₂{C(H)Ph₂}₂^{tBu}-2,6,4), and the *bis*(aryl) complexes Ar(Ar*)NGe(Cl) [Ar = Ph **142**, Mes **143**, C₆H₃-3,5-(CF₃)₂ **144**, Trip **145**].^{77,96} The germanium-centred free radical formed from the positive muon irradiation of **113** has been investigated by muon spin spectroscopy.⁹⁷ The spectrum is consistent with cyclohexadienyl radicals formed by competitive addition of muonium to the five aromatic rings of the ligand.

Halide abstraction reactions have afforded [Me₃Si(Ar*)NE][Al{OC(CF₃)₃}₄] (E = Ge **146**, Sn **147**), which feature a Group 14 cation.⁹⁸ The crystal structures of these complexes feature the metal centre coordinated to the monodentate [Me₃Si(Ar*)N][−] ligand, with an additional weak η²-interaction with a flanking aryl ring. Spectroscopic investigations indicate that these η²-interactions do not persist in solution on the NMR timescale. The ¹¹⁹Sn Mössbauer spectrum for **147** recorded at 78 K, exhibited an isomer shift of δ = 3.369(4) mm s^{−1}, consistent with a tin(II) atom and a large quadrupole splitting parameter showing a non-cubic environment around the tin centre.⁹⁹ Highlighting the electrophilic nature of these cations, complexation with DMAP occurs into the empty p orbital which is coplanar with the CNSiE (E = Ge, Sn) moiety, affording [Me₃Si(Ar*)NE(DMAP)][Al{OC(CF₃)₃}₄] (E = Ge **148**, Sn **149**, Figure 16).

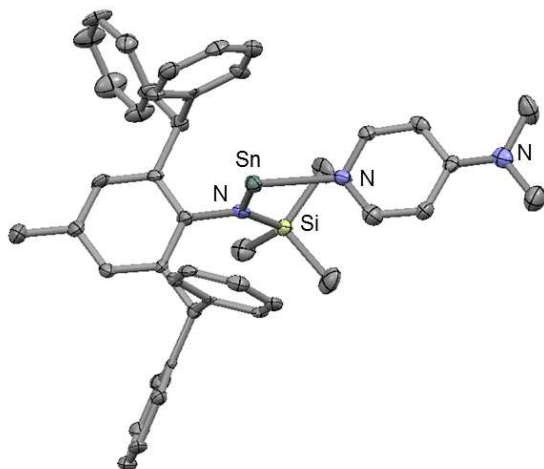
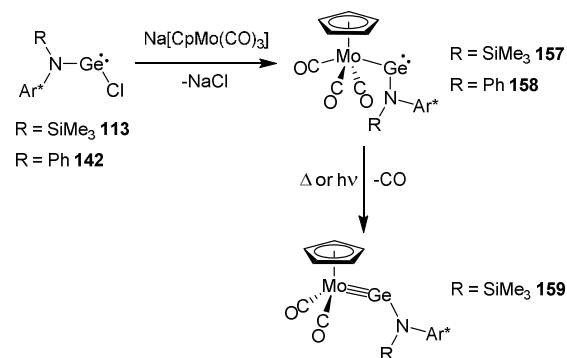


Figure 16 The molecular structure of the cationic component of $[\text{Me}_3\text{Si}(\text{Ar}^*)\text{NSn}(\text{DMAP})][\text{Al}\{\text{OC}(\text{CF}_3)_3\}_4]$ (**149**), with thermal ellipsoids set at 50%.⁹⁸ Hydrogen atoms are omitted for clarity.

The germylene $\text{Me}_3\text{Si}(\text{Ar}^*)\text{NGe}[\text{B}(\text{NDippCH})_2]$ (**150**) has been synthesised, along with related silylene and stannylene complexes.¹⁰⁰ By increasing the steric bulk of the amide ligand yet further, it is possible to isolate a monomeric hydrido-germylene.¹⁰¹ The reactions between $(^t\text{BuO})_3\text{Si}(\text{Ar})\text{NGe}(\text{O}^t\text{Bu})$ ($\text{Ar} = \text{Ar}^*$ **151**, Ar^\dagger **152**) and the borane HBcat ($\text{cat} = \text{catecholato}$, $\text{O}_2\text{C}_6\text{H}_4$) afforded the hydrido-germylenes $(^t\text{BuO})_3\text{Si}(\text{Ar})\text{NGe}(\text{H})$ ($\text{Ar} = \text{Ar}^*$ **153**, Ar^\dagger **154**) through σ -bond metathesis reactions. Displaying no intramolecular interactions with the oxygen atoms of the siloxy substituents or the flanking aryls, these complexes are the first structurally authenticated two-coordinate, primary tetrelenes [where $:\text{E}(\text{H})\text{R}$, $\text{E} = \text{C-Pb}$]. Calculations performed on **153** show that the dimerisation to the corresponding digermene or bridged hydride is endergonic by $3.1 \text{ kcal mol}^{-1}$ and $16.5 \text{ kcal mol}^{-1}$, respectively, with a small degree of $\text{N} \rightarrow \text{Ge}$ π -bonding to be contributing to this lack of dimerisation. The hydrido-germylene and stannylene complexes $^i\text{Pr}_3\text{Si}(\text{Ar}^\dagger)\text{NE}(\text{H})$ ($\text{E} = \text{Ge}$ **125**, Sn **155**) are efficient catalysts for the hydroboration of carbonyl compounds using HBpin ($\text{pin} = \text{pinacolato}$, $\text{O}_2\text{C}_2\text{Me}_4$) under relatively mild conditions and with low catalyst loadings.¹⁰² Reactions

involving the precatalyst ${}^i\text{Pr}_3\text{Si}(\text{Ar}^\dagger)\text{NSn}(\text{O}^t\text{Bu})$ (**156**) were more rapid than those for **125**, the increased activity attributed to a larger, more Lewis acidic centre and more polar $\delta^+\text{M}-\text{O}^{\delta-}$ bonds in the tin intermediates.

113 and **142** have been used to synthesise $\text{Cp}(\text{CO})_3\text{Mo}-\text{GeN}(\text{Ar}^*)\text{R}$ ($\text{Cp} = \eta^5\text{-C}_5\text{H}_5$, $\text{R} = \text{SiMe}_3$ **157**, Ph **158**) complexes through salt elimination reactions with $\text{Na}[\text{CpMo}(\text{CO})_3]$ (Scheme 9).⁷⁷ Unusually, these metalla-germylene complexes are resistant to CO elimination both in solution and the solid state, unlike the *m*-terphenyl analogue.¹⁰³ In the case of **157**, CO elimination can be initiated by heating a toluene solution at reflux for 1 hour, or by irradiating a benzene solution using UV light for 20 mins, yielding the metalla-germylyne $\text{Cp}(\text{CO})_2\text{Mo}\equiv\text{GeN}(\text{Ar}^*)\text{SiMe}_3$ (**159**). **159** features a Mo–Ge bond [2.2811(4) Å] which is significantly shorter than that in **157**, and it displays carbonyl stretching frequencies at 1926 and 1823 cm^{-1} , indicating a greater contribution from the germylyne than the heterovinylidene resonance form $\text{Cp}(\text{CO})_2^-\text{Mo}=\text{Ge}=\text{N}^+(\text{Ar}^*)\text{SiMe}_3$.

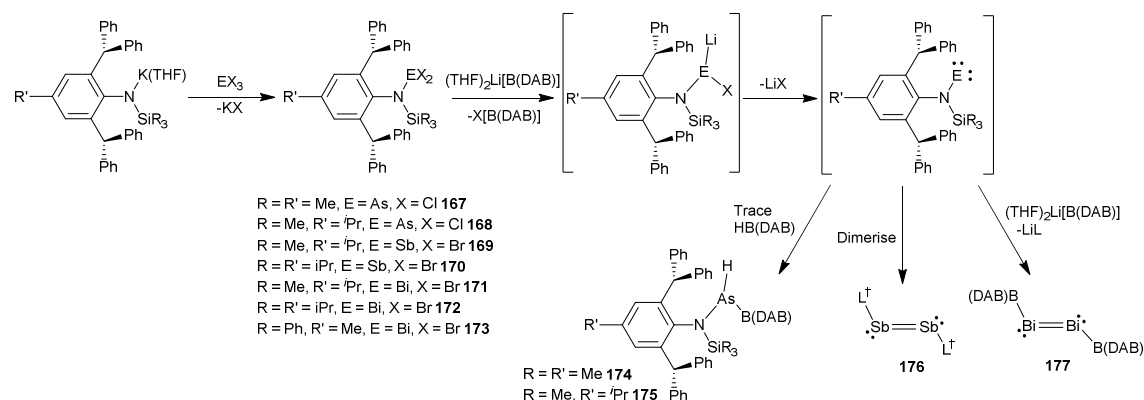


Scheme 9 The syntheses of $\text{Cp}(\text{CO})_3\text{Mo}-\text{GeN}(\text{Ar}^*)\text{R}$ ($\text{R} = \text{SiMe}_3$ **157**, Ph **158**) and $\text{Cp}(\text{CO})_2\text{Mo}\equiv\text{GeN}(\text{Ar}^*)\text{SiMe}_3$ (**159**).⁷⁷

4.4 Group 15 Complexes

Schulz and co-workers have utilised the $[\text{Me}_3\text{Si}(\text{Ar}^*)\text{N}]^-$ and $[\text{Me}_3\text{Si}(\text{Ar}^{t\text{Bu}})\text{N}]^-$ ligands to stabilise the "disguised" polarophiles $\text{Me}_3\text{Si}(\text{Ar}^*)\text{NECl}_2$ ($\text{E} = \text{Sb}$ **160**, Bi **161**) and $\text{Me}_3\text{Si}(\text{Ar}^{t\text{Bu}})\text{NBiCl}_2$ **162**, which can be used to synthesise the chlorostibonium and

bismuthenium complexes $[\text{Me}_3\text{Si}(\text{Ar})\text{NECl}][\text{Al}(\text{OCH}(\text{CF}_3)_2)_4]$ ($\text{Ar} = \text{Ar}^*$, $\text{E} = \text{Sb}$ **163**, Bi **164**; $\text{Ar} = \text{Ar}^{\text{tBu}}$, $\text{E} = \text{Bi}$ **165**) and $[\text{Me}_3\text{Si}(\text{Ar}^*)\text{NBi}(\text{Cl})][\text{GaCl}_4]$ (**166**), where the cations are stabilised by arene-element interactions.¹⁰⁴ In the case of the formation of **166** from **161** and GaCl_3 , no sign of a GaCl_3 -assisted Me/Cl exchange reaction was observed; this is in contrast to the *m*-terphenyl amides (see Section 2.4).^{53,54} The crystal structures of **163-165** and **166** show E=N double bonds, and the N–E–Cl angles [in the range $94.63(9)^\circ$ – $96.31(8)^\circ$] show that the Group 15 element lone pair is generally *s*-character. The reaction between **164** and DMAP led to the degradation of the aluminate anion and coordination of the $[\text{OCH}(\text{CF}_3)_2]^-$ ligand to the bismuth centre, with concomitant formation of $\text{DMAP}\cdot\text{Al}(\text{OCH}(\text{CF}_3)_2)_3$.



Scheme 10 The synthesis of and reactivity of amide-Group 15 element(III) dihalide complexes **167-173**.¹⁰⁵

A range of amide-group 15 element(III) dihalide complexes (**167-173**) have been synthesised, stabilised by these sterically demanding ligands (Scheme 10).¹⁰⁵ Reduction to the dipnictines was accomplished using the lithium boryl $(\text{THF})_2\text{Li}[\text{B}(\text{DAB})]$ [$\text{DAB} = (\text{NDippCH})_2$], although the products of these reactions were dependent on the nature of the Group 15 element and the bulk of the ligand. In the case of the arsenic complexes low yields of the amide/boryl arsines **174** and **175** could be identified out of the complex mixtures, in the case of **172**, ${}^i\text{Pr}_3\text{Si}(\text{Ar}^\dagger)\text{NSb}=\text{SbN}(\text{Ar}^\dagger)\text{Si}^i\text{Pr}_3$ (**176**), the first example of an amido distibene

was formed. For the bismuth complexes, use of the least bulky **171** afforded (DAB)BBi=BiB(DAB) (**177**), the first boryl dibismuthene. It is proposed that these reactions all proceed *via* the pnictinidene intermediates LE, which may form from lithium halide elimination from initial pnictinidenoid products (Scheme 10).

5. Summary and Outlook

The three classes of sterically demanding, monodentate amide ligands discussed herein – *m*-terphenyl anilide $[N(R)\{C_6H_3Ar_{2-2,6}\}]^-$, substituted carbazol-9-yl and $[N(R)(Ar')]^-$ ($Ar' = 2,6\text{-}\{C(H)Ph_2\}\text{-}4\text{-}R'\text{-}C_6H_2$) ligands, are proving very effective in the stabilisation of unusual and highly reactive bonding modes for the main group elements. An outstanding feature of these ligands is the ability to tune their steric demands which will further allow the tailoring of the resulting complexes for example coordination numbers and metal-metal bond orders. Examples of small molecule activation chemistry under mild conditions and catalysis have shown potential for a range of applications and this will no doubt continue to flourish. The use of extremely sterically demanding monodentate ligands to access main group complexes in low-coordination numbers and highly reactive bonding modes continues to be of intense research interest, and it is without doubt that these amide ligand families will be instrumental in driving this area forward.

6. References

1. M. F. Lappert, P. P. Power, A. V. Protchenko and A. L. Seeber, *Metal Amide Chemistry*, Wiley-VCH, Weinheim, 2009.
2. P. P. Power, *J. Organomet. Chem.*, 2004, **689**, 3904.
3. *The Group 13 Metals Aluminium, Gallium, Indium and Thallium. Chemical Patterns and Peculiarities*, A. J. Downs and S. Aldridge (ed.), Wiley-Blackwell, Chichester, 2011.

4. M. P. Coles, *Coord. Chem. Rev.*, 2015, **297-298**, 2.
5. M. P. Coles, *Coord. Chem. Rev.*, 2015, **297-298**, 24.
6. See, for example: (a) D. Mannig, H. Nöth, M. Schwartz, S. Weber and U. Wietelmann, *Angew. Chem. Int. Ed.*, 1985, **24**, 998; (b) A. M. Arif, A. H. Cowley, M. Pakulski and J. M. Power, *J. Chem. Soc., Chem. Commun.*, 1986, 889; (c) E. Crosbie, P. Garcia-Alvarez, A. R. Kennedy, J. Klett, R. E. Mulvey and S. D. Robertson., *Angew. Chem., Int. Ed.*, 2010, **49**, 9388; (d) C. -J. Maier, H. Pritzkow and W. Siebert, *Angew. Chem. Int. Ed.*, 1999, **38**, 1666; (e) E. Rivard, W. A. Meriall, J. C. Fettinger and P. P. Power, *Chem. Commun.*, 2006, 3800.
7. See, for example: (a) A. Meller, G. Ossig, W. Maringgele, D. Stalke, R. Herbst-Irmer, S. Freitag and G. M. Sheldrick, *J. Chem. Soc., Chem. Commun.*, 1991, 1123; (b) A Voigt, R. Murgavel, E. Parisini, H. W. Roesky, *Angew. Chem. Int. Ed.*, 1996, **35**, 748; (c) Y. Tang, A. M. Felix, L. N. Zarkharov, A. L. Rheingold and R. A. Kemp, *Inorg. Chem.*, 2004, **43**, 7239.
8. See, for example: (a) M. A. Petrie, K. Ruhlandt-Senge, P. P. Power, *Inorg. Chem.*, 1993, **32**, 1135; (b) S. D. Waezsada, T. Belghardt, M. Noltemeyer and H. W. Roesky, *Angew. Chem. Int. Ed.*, 1994, **33**, 1351; (c) K. Wraage, L. Lameyer, D. Stalke, H. W. Roesky, *Angew. Chem. Int. Ed.*, 1999, **38**, 522; (d) J. R. Babcock, L. Liable-Sands, A. L. Rheingold, L. R. Sita, *Organometallics*, 1999, **18**, 4437; (e) M. Brynda, R. Herber, P. B. Hitchcock, M. F. Lappert, I. Nowick, P. P. Power, A. V. Protchenko, A. Ruzicka and J. Steiner, *Angew. Chem. Int. Ed.*, 2006, **45**, 4333.
9. See, for example: (a) N. Burford, T. S. Cameron, C. L. B. Macdonald, K. N. Robertson, R. Schurko, D. Walsh, R. McDonald and R. E. Wasylshen, *Inorg. Chem.*, 2005, **44**, 8085; (b) M. Lehmann, A. Schulz and A. Villinger, *Eur. J. Inorg. Chem.*, 2010, 5501.

10. See, for example: (a) M. A. Petrie, K. Ruhlandt-Senge and P. P. Power, *Inorg. Chem.*, 1993, **32**, 1135; (b) K. M. Waggoner, K. Ruhlandt-Senge, R. J. Wehmschulte, X. He, M. M. Olmstead and P. P. Power, *Inorg. Chem.*, 1993, **32**, 2557; (c) Y. Tang, L. N. Zarkharov, A. L. Rheingold and R. A. Kemp, *Organometallics*, 2005, **24**, 836.
11. J. Barker and M. Kilner, *Coord. Chem. Rev.*, 1994, **133**, 219.
12. F. T. Edelmann, *Coord. Chem. Rev.*, 1994, **137**, 403.
13. P. J. Bailey and S. Pace, *Coord. Chem. Rev.*, 2001, **214**, 91.
14. N. J. Hardman, A. D. Phillips, P. P. Power, *ACS Symposium Series (Group 13 Chemistry)*, 2002, **822**, 2.
15. J. A. R. Schmidt and J. Arnold, *J. Chem. Soc., Dalton Trans.*, 2002, 2890.
16. L. Bourget-Merle, M. F. Lappert and J. R. Severn, *Chem. Rev.*, 2002, **102**, 3031.
17. I. Saur, S. G. Alonso, J. Barrau, *Appl. Organomet. Chem.*, 2005, **19**, 414.
18. L. Bourget-Merle, Y. Cheng, D. J. Doyle, P. B. Hitchcock, A. V. Khvostov, M. F. Lappert, A. V. Protchenko, X. Wei, *ACS Symposium Series (Modern Aspects of Main Group Chemistry)*, 2006, **917**, 192.
19. P. C. Junk, M. L. Cole, *Chem. Commun.*, 2007, 1579.
20. F. T. Edelmann, *Adv. Organomet. Chem.*, 2008, **57**, 183.
21. S. Nagendran and H. W. Roesky, *Organometallics*, 2008, **27**, 457.
22. C. Jones, *Coord. Chem. Rev.*, 2010, **254**, 1273.
23. S. P. Sarish, S. Nembenna, S. Nagendran, H. W. Roesky, *Acc. Chem. Res.*, 2011, **44**, 157.
24. A. Stasch, C. Jones, *Dalton Trans.*, 2011, **40**, 5659.
25. S. T. Barry, *Coord. Chem. Rev.*, 2013, **257**, 3192.
26. (a) P. P. Power, *J. Chem. Soc., Dalton Trans.* **1998**, 2939; (b) B. Twamley, S. T. Haubrich P. P. Power, *Adv. Organomet. Chem.* **1999**, *44*, 1; (c) J. A. C. Clyburne, N. McMullen, *Coord. Chem. Rev.* **2000**, *210*, 73; (d) P. P. Power, *Struct. Bond. (Berlin)* **2002**, *103*, 57.

- (d) P. P. Power, *Chem. Rev.*, 2003, **103**, 789; (e) P. P. Power, *Appl. Organomet. Chem.*, 2005, **19**, 488; (f) P. P. Power, *Organometallics* **2007**, **26**, 4362; (g) E. Rivard, P. P. Power, *Inorg. Chem.* **2007**, **46**, 10047; (h) E. Rivard, P. P. Power, *Dalton Trans.*, **2008**, 33, 4336; (i) D. L. Kays, *Organomet. Chem.* **2010**, **36**, 56; (j) C. Ni, P. P. Power, *Struct. Bond. (Berlin)* **2010**, **136**, 59; (k) D. L. Kays, *Dalton Trans.* **2011**, **40**, 769.
27. B. Twamley, C.-S. Hwang, N. J. Hardman, P. P. Power, *J. Organomet. Chem.*, 2000, **609**, 152.
28. R. J. Wright, J. Steiner, S. Beaini, P. P. Power, *Inorg. Chim. Acta*, 2006, **359**, 1939.
29. See, for example: (a) J. Gavenonis and T.D. Tilley, *Organometallics*, 2002, **21**, 5549; (b) J. Gavenonis and T.D. Tilley, *J. Am. Chem. Soc.*, 2002, **124**, 8536; (c) C. Ni, J. C. Fettinger, G. J. Long and P. P. Power, *Inorg. Chem.*, 2009, **48**, 2443; (d) C. Ni, B. Rekken, J. C. Fettinger, G. J. Long and P. P. Power, *Dalton Trans.*, 2009, 8349; (e) V. M. Iluc and G. L. Hillhouse, *J. Am. Chem. Soc.*, 2010, **132**, 15148; (f) J. N. Boynton, J.-D. Guo, J. C. Fettinger, C. E. Melton, S. Nagase and P. P. Power, *J. Am. Chem. Soc.*, 2013, **135**, 10720; (g) J. N. Boynton, J.-D. Guo, F. Grandjean, J. C. Fettinger, S. Nagase, G. J. Long and P. P. Power, *Inorg. Chem.*, 2013, **52**, 14216; (h) J. C. Axtell, R. R. Schrock, P. Müller, and A. H. Hoveyda, *Organometallics*, 2015, **34**, 2110; (i) C. B. Hansen, R. F. Jordan and G. L. Hillhouse, *Inorg. Chem.*, 2015, **54**, 4603.
30. P.L. Arnold, S.T. Liddle, *C. R. Chimie*, 2008, **11**, 603.
31. H. Zhu, J. Chai, V. Chandrasekhar, H. W. Roesky, J. Magull, D. Vidovic, H.-G. Schmidt, M. Noltemeyer, P. P. Power and W. A. Merrill, *J. Am. Chem. Soc.*, 2004, **126**, 9472.
32. N. J. Hardman, C. Cui, H. W. Roesky, W. H. Fink and P. P. Power, *Angew. Chem. Int. Ed.*, 2001, **40**, 2172.
33. R. J. Wright, A. D. Phillips, T. L. Allen, W. H. Fink and P. P. Power, *J. Am. Chem. Soc.*, 2003, **125**, 1694.

34. H. Zhu, J. Chai, V. Jancik, H. W. Roesky, W. A. Merrill and P. P. Power, *J. Am. Chem. Soc.*, 2005, **127**, 10170.
35. E. Rivard, W. A. Merrill, J. C. Fettinger, R. Wolf, G. H. Spikes and P. P. Power, *Inorg. Chem.*, 2007, **46**, 2971.
36. R. J. Wright, M. Brynda and P. P. Power, *Inorg. Chem.*, 2005, **44**, 3368.
37. R. J. Wright, M. Brynda, J. C. Fettinger, A. R. Betzer and P. P. Power, *J. Am. Chem. Soc.*, 2006, **128**, 12498.
38. R. S. Ghadwal, H. W. Roesky, C. Schulzke and M. Granitzka, *Organometallics*, 2010, **29**, 6329.
39. R. S. Ghadwal, H. W. Roesky, K. Pröpper, B. Dittrich, S. Klein, and G. Frenking, *Angew. Chem. Int. Ed.*, 2011, **50**, 5374.
40. R. S. Ghadwal, R. Azhakar, K. Pröpper, B. Dittrich and M. John, *Chem. Commun.*, 2013, **49**, 5987.
41. P. P. Samuel, R. Azhakar, R. S. Ghadwal, S. S. Sen, H. W. Roesky, M. Granitzka, J. Matussek, R. Herbst-Irmer and D. Stalke, *Inorg. Chem.*, 2012, **51**, 11049.
42. D. Bubrin and M. Niemeyer, *Inorg. Chem.*, 2014, **53**, 1269.
43. W. A. Merrill, R. J. Wright, C. S. Stanciu, M. M. Olmstead, J. C. Fettinger and P. P. Power, *Inorg. Chem.*, 2010, **49**, 7097.
44. D. Michalik, A. Schulz, A. Villinger and N. Weding, *Angew. Chem. Int. Ed.*, 2008, **47**, 6465.
45. A. Schulz and A. Villinger, *Inorg. Chem.*, 2009, **48**, 7359.
46. D. Michalik, A. Schulz and A. Villinger, *Angew. Int. Ed. Engl.*, 2010, **49**, 7575.
47. F. Reiß, A. Schulz, A. Villinger and N. Weding, *Dalton Trans.*, 2010, **39**, 9962.
48. M. Lehmann, A. Schulz and A. Villinger, *Angew. Chem. Int. Ed.*, 2012, **51**, 8087.
49. A. Schulz, A. Villinger and A. Westenkirchner, *Inorg. Chem.*, 2013, **52**, 11457.

50. T. Beweries, R. Kuzora, U. Rosenthal, A. Schulz and A. Villinger, *Angew. Chem. Int. Ed.*, 2011, **50**, 8974.
51. S. Demeshko, C. Godemann, R. Kuzora, A. Schulz and A. Villinger, *Angew. Chem. Int. Ed.*, 2013, **52**, 2105.
52. A. Schulz, A. Villinger, *J. Organomet. Chem.* 2007, **692**, 2839.
53. D. Michalik, A. Schulz, and A. Villinger, *Inorg. Chem.*, 2008, **47**, 11798.
54. C. Hering, M. Lehmann, A. Schulz and A. Villinger, *Inorg. Chem.*, 2012, **51**, 8212.
55. F. Reiß, A. Schulz and A. Villinger, *Eur. J. Inorg. Chem.*, 2012, 261.
56. (a) Y. Miura and Akio Tanaka, *J. Chem. Soc., Chem. Commun.*, 1990, 441; (b) Y. Miura, T. Fuchikami, M. Momoki, *Chem. Lett.*, 1994, 2127; (c) Y. Miura, M. Momoki and T. Fuchikami, *J. Org. Chem.*, 1996, **61**, 4300; (d) Y. Miura and T. Tomimura, *J. Org. Chem.*, 2000, **65**, 7889; (e) Y. Miura, Y. Oyama and Y. Teki, *J. Org. Chem.*, 2003, **68**, 1225; (f) Y. Miura, I. Katoa and Y. Teki, *Dalton Trans.*, 2006, 961.
57. S. Sasaki, H. Hatsushiba and M. Yoshifuji, *J. Chem. Soc., Chem. Commun.*, 1998, 2221.
58. R. Dinnebier, H. Esbak, F. Olbrich and U. Behrens, *Organometallics*, 2007, **26**, 2604.
59. H.-C. Gee, C.-H. Lee, Y.-H. Jeong and W.-D. Jang, *Chem. Commun.*, 2011, **47**, 11963.
60. J. A. Gaunt, V. C. Gibson, A. Haynes, S. K. Spitzmesser, A. J. P. White and D. J. Williams, *Organometallics*, 2004, **23**, 1015.
61. M. Inoue, T. Suzuki and M. Nakada, *J. Am. Chem. Soc.*, 2003, **125**, 1140.
62. T. Niwa and M. Nakada, *J. Am. Chem. Soc.*, 2012, **134**, 13538.
63. I. V. Basalov, S. C. Roşca, D. M. Lyubov, A. N. Selikhov, G. K. Fukin, Y. Sarazin, J.-F. Carpentier and A. A. Trifonov, *Inorg. Chem.*, 2014, **53**, 1654.
64. N. D. Coombs, A. Stasch, A. Cowley, A. L. Thompson and S. Aldridge, *Dalton Trans.*, 2008, 332.
65. F. Neugebauer, H. Fischer, *Angew. Chem. Int. Ed. Engl.*, 1971, **10**, 732.

66. S. K. Spitzmesser and V. C. Gibson, *J. Organomet. Chem.*, 2003, **673**, 95.
67. H. B. Mansaray, M. Kelly, D. Vidovic and S. Aldridge, *Chem. Eur. J.*, 2011, **17**, 5381.
68. R. S. Moorhouse, G. J. Moxey, F. Ortu, T. J. Reade, W. Lewis, A. J. Blake and D. L. Kays, *Inorg. Chem.*, 2013, **52**, 2678.
69. A. J. Blake, W. Lewis, J. McMaster, R. S. Moorhouse, G. J. Moxey and D. L. Kays, *Dalton Trans.*, 2011, **40**, 1641.
70. R. Hacker, E. Kauffmann, P. v. R. Schleyer, W. Mahdi, H. Dietrich, *Chem. Ber.*, 1987, **120**, 1533.
71. A. E. Ashley, A. R. Cowley, J. C. Green, D. R. Johnston, D. J. Watkin and D. L. Kays, *Eur. J. Inorg. Chem.*, 2009, 2547.
72. F. Ortu, G. J. Moxey, A. J. Blake, W. Lewis and D. L. Kays, *Chem. Eur. J.*, 2015, **21**, 6949.
73. N. Kuhn, M. Schulten, R. Boese and D. Bläser, *J. Organomet. Chem.*, 1991, **421**, 1.
74. A. N. Selikhov, A. V. Cherkasov, G. K. Fukin, A. A. Trifonov, I. del Rosal and L. Maron, *Organometallics*, 2015, **34**, 555.
75. G. Berthon-Gelloz, M. A. Siegler, A. L. Spek, B. Tinant, J. N. H. Reek and I. Markó, *Dalton Trans.*, 2010, **39**, 1444.
76. J. Li, A. Stasch, C. Schenk and C. Jones, *Dalton Trans.*, 2011, **40**, 10448.
77. J. Hicks, T. J. Hadlington, C. Schenk, J. Li and C. Jones, *Organometallics*, 2013, **32**, 323.
78. T. J. Hadlington, J. Li and C. Jones, *Can. J. Chem.*, 2014, **92**, 427.
79. E. W. Y. Wong, D. Dange, L. Fohlmeister, T. J. Hadlington and C. Jones, *Aust. J. Chem.*, 2013, **66**, 1144.
80. J. Hicks, Chad E. Hoyer, B. Moubaraki, G. Li Manni, E. Carter, D. M. Murphy, K. S. Murray, L. Gagliardi and C. Jones, *J. Am. Chem. Soc.*, 2014, **136**, 5283.
81. D. Dange, J. Li, C. Schenk, H. Schnöckel, C. Jones, *Inorg. Chem.*, 2012, **51**, 13050.

82. A. V. Protchenko, D. Dange, J. R. Harmer, C. Y. Tang, A. D. Schwarz, M. J. Kelly, N. Phillips, R. Tirfoin, K. Hassomal Birjkumar, C. Jones, N. Kaltsoyannis, P. Mountford and S. Aldridge, *Nat. Chem.*, 2014, **6**, 315.
83. V. Chandrasekhar, S. Nagendran, R. Boomishankar and R. J. Butcher, *Inorg. Chem.*, 2001, **40**, 940.
84. Y. Peng, R. C. Fischer, W. A. Merrill, J. Fischer, L. Pu, B. D. Ellis, J. C. Fettinger, R. H. Herber and P. P. Power, *Chem. Sci.*, 2010, **1**, 461 and references therein.
85. J. Li, C. Schenk, C. Goedecke, G. Frenking and C. Jones, *J. Am. Chem. Soc.*, 2011, **133**, 18622.
86. A. Sekiguchi, *Pure Appl. Chem.*, 2008, **80**, 447.
87. M. Hermann, C. Goedecke, C. Jones and G. Frenking, *Organometallics*, 2013, **32**, 6666.
88. M. Hermann, C. Jones and G. Frenking, *Inorg. Chem.*, 2014, **53**, 6482.
89. J. Li, M. Hermann, G. Frenking and C. Jones, *Angew. Chem. Int. Ed.*, 2012, **51**, 8611.
90. C. Cui, M. M. Olmstead, J. C. Fettinger, G. H. Spikes and P. P. Power, *J. Am. Chem. Soc.*, 2005, **127**, 17530.
91. T. J. Hadlington, M. Hermann, J. Li, G. Frenking and C. Jones, *Angew. Chem. Int. Ed.*, 2013, **52**, 10199.
92. G. H. Spikes, J. C. Fettinger and P. P. Power, *J. Am. Chem. Soc.*, 2005, **127**, 12232.
93. T. J. Hadlington and C. Jones, *Chem. Commun.*, 2014, **50**, 2321.
94. Y. Peng, X. Wang, J. C. Fettinger and P. P. Power, *Chem. Commun.*, 2010, **46**, 943.
95. (a) L. Pu, M. M. Olmstead, P. P. Power and B. Schiemenz, *Organometallics*, 1998, **17**, 5602; (b) B. E. Eichler, L. Pu, M. Stender and P. P. Power, *Polyhedron*, 2001, **20**, 551.
96. T. J. Hadlington, J. Li and C. Jones, *Can. J. Chem.*, 2014, **92**, 427.
97. R. West, K. Samedov, A. Mitra, P. W. Percival, J.-C. Brodovitch, G. Langille, B. M. McCollum, T. Iwamoto, S. Ishada, C. Jones and J. Li, *Can. J. Chem.*, 2014, **92**, 508.

98. J. Li, C. Schenk, F. Winter, H. Scherer, N. Trapp, A. Higelin, S. Keller, R. Pöttgen, I. Krossing and C. Jones, *Angew. Chem. Int. Ed.*, 2012, **51**, 9557.
99. (a) P. E. Lippens, *Phys. Rev. B*, 1999, **60**, 4576; (b) C. L. Macdonald, R. Bandyopadhyay, B. F. T. Cooper, W. W. Friedl, A. J. Rossini, R. W. Schurko, S. H. Eichhorn and R. H. Herber, *J. Am. Chem. Soc.*, 2012, **134**, 4332.
100. A. V. Protchenko, K. Hassomal Birjkumar, D. Dange, Andrew D. Schwarz, D. Vidovic, C. Jones, N. Kaltsoyannis, P. Mountford and S. Aldridge, *J. Am. Chem. Soc.*, 2012, **134**, 6500.
101. T. J. Hadlington, B. Schwarze, E. I. Izgorodina and C. Jones, *Chem. Commun.*, 2015, **51**, 6854.
102. T. J. Hadlington, M. Hermann, G. Frenking and C. Jones, *J. Am. Chem. Soc.*, 2014, **136**, 3028.
103. R. S. Simons and P. P. Power, *J. Am. Chem. Soc.*, 1996, **118**, 11966.
104. C. Hering-Junghans, M. Thomas, A. Villinger and A. Schulz, *Chem. Eur. J.*, 2015, **21**, 6713.
105. D. Dange, A. Davey, J. A. B. Abdalla, S. Aldridge and C. Jones, *Chem. Commun.*, 2015, **51**, 7128.